Internal state configures olfactory behavior and early sensory processing in *Drosophila* larva

Katrin Vogt[1,2,*], David M. Zimmerman[1,2,3], Matthias Schlichting[4], Luis Hernandez-Nuñez[1,2,5], Shanshan Qin[6], Karen Malacon[1,2], Michael Rosbash[4], Cengiz Pehlevan[2,6], Albert Cardona[7], and Aravinthan D.T. Samuel[1,2,*]

[1]Department of Physics, Harvard University, Cambridge, MA 02138, USA, [2]Center for Brain Science, Harvard University, Cambridge, MA 02138, USA, [3]Harvard Graduate Program in Biophysics, Harvard University, Cambridge, MA 02138, USA, [4]Howard Hughes Medical Institute and National Center for Behavioral Genomics, Brandeis University, Waltham, MA 02454, USA, [5]Center for Systems Biology, Harvard University, Cambridge, MA 02138, USA, [6]John A. Paulson School of Engineering and Applied Sciences, Harvard University, Cambridge, MA 02138, USA, [7]Howard Hughes Medical Institute, Janelia Research Campus, Ashburn, VA 20147, USA

Animals can respond differently to a sensory cue when in different states. Here, we show that certain odors repel well-fed *Drosophila* larvae but attract food-deprived larvae and how feeding state flexibly alters neural processing in an early olfactory circuit, the antennal lobe, to determine the behavioral valence of a sensory cue. Odor valence is assigned by a neuronal architecture that controls a switch between two separate projection neuron output pathways that mediate opposite behavioral responses. A uniglomerular projection neuron pathway mediates odor attraction whereas a multiglomerular projection neuron pathway mediates odor repulsion. The serotonergic CSD neuron in the antennal lobe is a critical regulator of this neuronal and behavioral switch. CSD selects an appropriate behavior by shifting patterns of serotonergic modulation and glutamatergic inhibition onto each output pathway. The antennal lobe is a decision-making circuit for innate behavioral responses that uses feeding state to determine an odor's valence.

***For correspondence:** *katrinvogt@fas.harvard.edu* **(KV);** *samuel@physics.harvard.edu* **(ADTS)**

Keywords: neuromodulation, connectomics, *Drosophila* larva, olfaction, serotonin, antennal lobe

Introduction

An animal makes different decisions about food-related cues when it is hungry versus when it is well fed. Well-fed animals might use cues to be selective about food choices, whereas animals facing starvation might use such cues to find any available food (Wu et al., 2005; Inagaki et al., 2014; Crossley et al., 2018). Olfactory responses are naturally modulated by feeding state, as many animals use odors to identify food. In adult *Drosophila*, food deprivation affects different levels of olfactory processing, e.g., modulation of the excitability of olfactory receptor neurons (ORNs) or modulation of brain regions for sleep-wake cycles and feeding (Root et al., 2011; Ko et al., 2015; Wang et al., 2013; Chung et al., 2017). However, the fixed architecture of the antennal lobe, the first olfactory center in *Drosophila*, is thought to have a stereotyped role in formatting sensory inputs for use by downstream circuits (Olsen and Wilson, 2008).

We asked how the small olfactory circuit of the *Drosophila* larva might use internal state to select an innate behavioral response to an odor. The larval olfactory circuit has only 21 different ORNs, each expressing a different receptor and innervating a distinct glomerulus in the larval antennal lobe (lAL). The complete connectome of the lAL has been mapped by serial-section electron microscopy (Berck et al., 2016). One striking but poorly understood feature of the lAL is that two different sets of projection neurons convey output from its glomeruli to higher brain areas. Each uniglomerular projection neuron (uPN) directly relays information from a single ORN to the mushroom body (MB) calyx and the lateral horn (LH) (Masuda-Nakagawa et al., 2009). Each of 14 multiglomerular projection neurons (mPN) receives input from a different subset of ORNs and sends its output to different brain regions (Berck et al., 2016).

We discovered that the behavioral valence exhibited by *Drosophila* larvae to an odor can depend on feeding state. For example, geranyl acetate (GA), which is innately aversive to a fed larva, is attractive to a food-deprived larva. We demonstrate that this behavioral switch is computed within the lAL circuitry. The lAL contains a prominent serotonergic neuron (CSD) that is common to the larvae and adults of many insect species (Kent et al., 1987; Kloppenburg et al., 1999; Python and Stocker, 2002; Dacks et al., 2006; Roy et al., 2007). We show that serotonergic signals from CSD are used to shift the relative activity of an mPN pathway that mediates odor repulsion and an uPN pathway that mediates attraction. A small number of glutamatergic local interneurons also connects in different ways to these two sets of projection neurons (Olsen and Wilson, 2008; Liou et al., 2018). Using both this local glutamatergic inhibition as well as serotonergic modulation, CSD shifts the relative activation of the mPN and uPN pathways by state-dependent regulation. This regulatory architecture effectively integrates sensory input, neuromodulation, and synaptic inhibition to determine the valence of an odor. Serotonergic neuromodulation underlies numerous state-dependent behaviors including aggression, circadian rhythms, and feeding behaviors (Johnson et al., 2009; Nichols, 2007; Neckameyer et al., 2007; Schoofs et al., 2018). Here, we show how the behavioral valence of an odor is shaped by neuromodulation within an early sensory circuit.

Results

Feeding state determines the behavioral valence of an odor

Food deprivation can alter food choice behaviors. A starving animal might assign positive valence to food cues that a fed animal would avoid or ignore. To test this possibility in *Drosophila* larva, we investigated their olfactory behavior in different feeding states. Most monomolecular odors are innately attractive to fed larvae. We screened a broad panel of such odors, and found two – geranyl acetate (GA) and menthol – that evoke avoidance in fed larvae but attraction in food-deprived larvae (Fig. 1A/B; S1A/B). Both GA and menthol are found in green leaves, which are not the larva's preferred food (Ganjewala and Luthra, 2009). Thus, innate avoidance in fed larvae and innate attraction in food-deprived larvae may reflect state-dependent food choice

behaviors.

We also tested the behavioral response to ethyl acetate (EA), an innately attractive odor to fed larvae. While we did not observe a change in the sign of behavioral valence, food-deprived larvae are significantly more attracted to EA (Fig. S1C). Mutant larvae ($Orco^{-/-}$) that lack functional ORNs are neither attracted nor repelled by GA, menthol, or EA when either fed or food-deprived (Fig. 1B; S1B/C). The state-dependent change in the behavioral valence of these odors requires the olfactory system.

Feeding state modulates the relative activity of lAL output pathways

The state-dependent switch in olfactory behavior to GA occurs over different odor concentrations and across different larval stages after 5-7 hours of food deprivation (Fig. S2A-C). The larval ORNs that are most sensitive to GA are those that express Or82a and Or45a (Si et al., 2019). Each ORN connects to one uPN that innervates the MB calyx and LH (Fig. 1C). The *GH146-GAL4* line (Masuda-Nakagawa et al., 2009) drives expression in all uPNs activated by GA (Fig. S2E). From the wiring diagram of the lAL, we also identified an mPN called "cobra" that receives direct synaptic input from several ORNs including those activated by GA (Fig. 1D). Cobra mPN projects to the vertical lobe of the mushroom bodies (Berck et al., 2016). We also identified a driver line (*GMR32E02-GAL4*) specific for cobra mPN expression (Fig. S2F).

To test whether the uPN or cobra mPN contribute to innate olfactory behavior to GA, we inactivated each pathway by expression of Kir2.1. uPN inactivation made food-deprived larvae unable to switch their behavioral responses from avoidance to attraction (Fig. 1C). In contrast, cobra inactivation caused fed larvae to be attracted to GA without affecting attraction in food-deprived larvae (Fig. 1D).

We next used calcium imaging to determine whether feeding state affects the relative activity of GA-sensing ORNs, uPNs, and the cobra mPN. First, we quantified odor-evoked activity in ORN axon terminals using calcium imaging in immobilized, intact larvae (Si et al., 2019). We expressed GCaMP6m either specifically in ORN-Or82a or ORN-Or45a or in all ORNs (Fig. 1E; S2D). We found no difference in odor-evoked ORN activity before or after food deprivation. However, we found that food deprivation both elevated the odor-evoked uPN response and reduced the odor-evoked mPN response (Fig. 1F/G; S2E/F).

These observations suggest that olfactory valence might be computed within the antennal lobe circuit, changing how a fixed ORN input is translated into the relative strength of its uPN and mPN output pathways (Fig. 1H). Higher uPN and lower mPN activity correlates with GA attraction. Lower uPN and higher mPN activity correlates with GA aversion. Because every odor activates different subsets of ORNs, uPNs, and mPNs, we focused this study on GA to dissect the mechanisms underlying this behavioral switch in the lAL (Si et al., 2019).

The mPN pathway receives glutamatergic inhibition in food-deprived larvae

We sought synaptic mechanisms within the lAL that might modulate the uPN and cobra mPN pathways. Glutamatergic local interneurons have been discovered in the wiring diagram that make many synapses onto the mPNs (Berck et al., 2016). Moreover, GluClα, a glutamate-gated chloride channel that makes glutamate inhibitory, is widely expressed in the adult antennal lobe (Liu and Wilson, 2013).

When we reduced GluClα expression specifically in cobra mPN, both fed and food-deprived animals exhibited GA avoidance (Fig. 2A). We imaged calcium dynamics in cobra mPN after GluClα knockdown, and also found no change in GA-evoked calcium dynamics between fed and food-deprived animals (Fig. 2B/C; S3A). Removing glutamatergic inhibition of cobra mPN appears to prevent inactivation of the odor avoidance pathway after food deprivation and behavioral valence is not shifted to attraction.

The glutamatergic local interneurons that innervate cobra mPN and receive input from GA-sensitive ORNs include four picky local interneurons (pLN0, pLN1, pLN2, and pLN4) (Berck et al., 2016). The wiring diagram only contains one other picky local interneuron type (pLN3) that neither innervates cobra mPN nor receives input from GA-sensitive ORNs. We obtained three cell-specific split GAL4 lines for pLN1, pLN3, and pLN4 (Fig. 2D; S3B-G). Cell-specific inactivation of pLN1, pLN3, or pLN4 had no effect on GA avoidance in fed larvae, but inactivating either pLN1 or pLN4 eliminated GA attraction in food-deprived larvae (Fig. 2E; S3H). With imaging, we found that GA-evoked calcium dynamics in pLN1 were elevated in the food-deprived state and undetectable in the fed state (Fig. 2F; S3I). We conclude that food deprivation may downregulate the cobra mPN pathway by increasing glutamatergic inhibition from pLN1 and pLN4 (Fig. 2G).

uPNs receive non-synaptic excitation through the 5-HT7 serotonin receptor

How might the activity of the uPN pathway be upregulated in food-deprived animals? The GABAergic and glutamatergic interneurons that synapse onto uPNs are thought to be inhibitory. However, serotonin can be a prominent neuromodulator, and the excitatory 5-HT7 receptor is expressed in the uPN pathway (Huser et al., 2017; Saudou et al., 1992) (Fig. 3A; S4A). We found that inactivating 5-HT7 expressing neurons did not impair GA avoidance in fed animals, consistent with previous observations (Huser et al., 2017) (Fig. 3B). However, inactivating 5-HT7 expressing neurons caused food-deprived larvae to avoid GA, similar to the phenotype obtained by inactivating all uPNs. We also specifically removed 5-HT7 from the uPN pathway using a CRISPR/Cas9-based cell type-specific gene knockout system (Schlichting et al., 2019; Delventhal et al., 2019). Without 5-HT7 in the uPNs, food-deprived larvae also avoided GA (Fig. 3C). With imaging, we found that odor-evoked calcium activity in the uPNs lacking 5-HT7 was weak in both food-deprived and fed animals (Fig. 3D/E; S4B). We conclude that serotonin is required by food-deprived animals to elevate odor-evoked uPN activity and shift behavioral valence to attraction.

Serotonin released from CSD changes odor valence

A single serotonergic neuron type called CSD spans both antennal lobes and innervates higher brain regions in the larva and adult fly (Dacks et al., 2006; Roy et al., 2007; Zhang and Gaudry, 2016; Huser et al., 2012) (Fig. 3F; S4C). We found that cell-specific inactivation of CSD using *R60F02-GAL4* (but not inactivation of other serotonergic neurons, Fig. S4D) causes GA avoidance in both fed and food-deprived larvae (Fig. 3G).

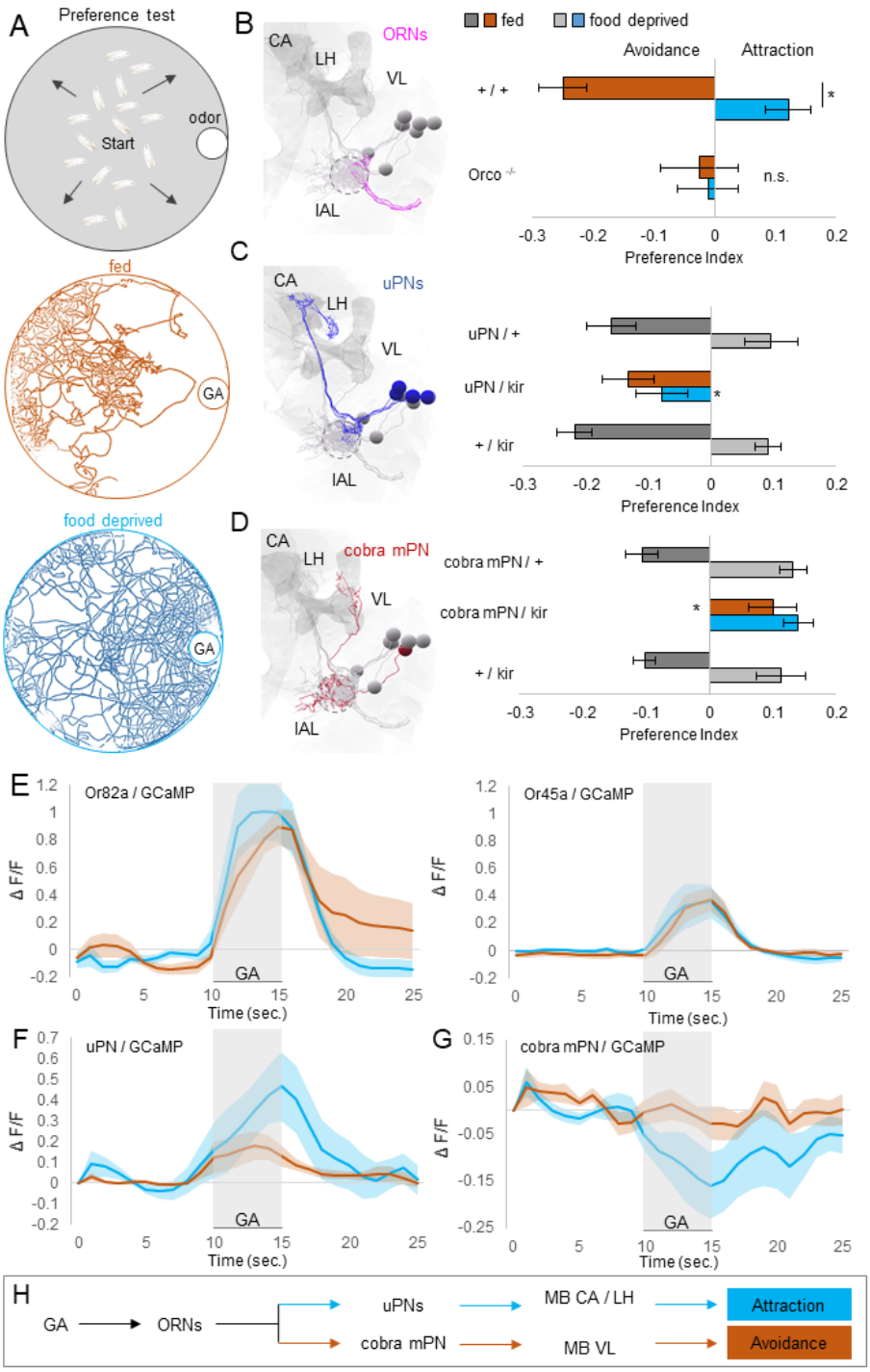

Figure 1. Feeding state determines the behavioral valence of GA by modulating different IAL output pathways in opposite directions. **A** Behavioral setup to test olfactory preference. 15 larvae start in the middle of the arena and are free to move in the presence of an odor source. In the fed state, larvae avoid GA. Food deprived larvae are attracted to GA. Colored lines represent all larval tracks over $15\,\mathrm{min}$. **B** Larvae show significant avoidance to GA in fed state (one sample t-test, $p < 0.001$) and significant attraction to GA in food deprived state (one sample t-test, $p < 0.01$). They show a significant switch from aversion to attraction upon food deprivation (two-sample t-test, $p < 0.001$). Mutant larvae (*Orco*$^{-/-}$) that lack functional ORNs do not respond to the odor in any state (one sample t-test, $p > 0.05$) ($n = 12$–18). **C** Blocking neuronal output of uPNs (*GH146-GAL4*) by expressing *UAS-Kir2.1* impairs the food deprived (one-way ANOVA, post-hoc pairwise comparison, $p < 0.05$) but not fed (one-way ANOVA, $p > 0.05$) odor response. ($n = 8$–10). **D** Blocking neuronal output of the cobra mPN by expressing *UAS-Kir2.1* under the control of *GMR32E03-GAL4* impairs avoidance in fed state (one-way ANOVA, post-hoc pairwise comparison, $p < 0.001$), but not attraction in food deprived state (one-way ANOVA, $p > 0.05$). ($n = 6$–10). **E** Calcium activity of the Or82a/Or45a neuron in response to GA (10^{-6}) in fed and food deprived larvae. Odor was presented for $5\,\mathrm{s}$. ORNs show the same activity levels in both states ($n = 5$–6).**F** Calcium activity in the uPNs in response to GA (10^{-6}). Odor was presented for $5\,\mathrm{s}$. uPNs show weak response in the fed state and an increased response after food deprivation ($n = 7$–9). **G** Calcium activity in the cobra mPN in response to GA (10^{-6}). Odor was presented for $5\,\mathrm{s}$. The cobra mPN shows decreased activity in the food deprived state ($n = 8$–9). **H** Two different IAL output pathways show different state dependent modulation and are required for different olfactory behaviors, respectively. Bar graphs represent pooled data from $5\,\mathrm{min}$ to $15\,\mathrm{min}$ during testing (mean $\pm$ SEM). Abbreviations: CA, mushroom body calyx; IAL, larval antennal lobe; LH, Lateral Horn; VL, mushroom body vertical lobe.

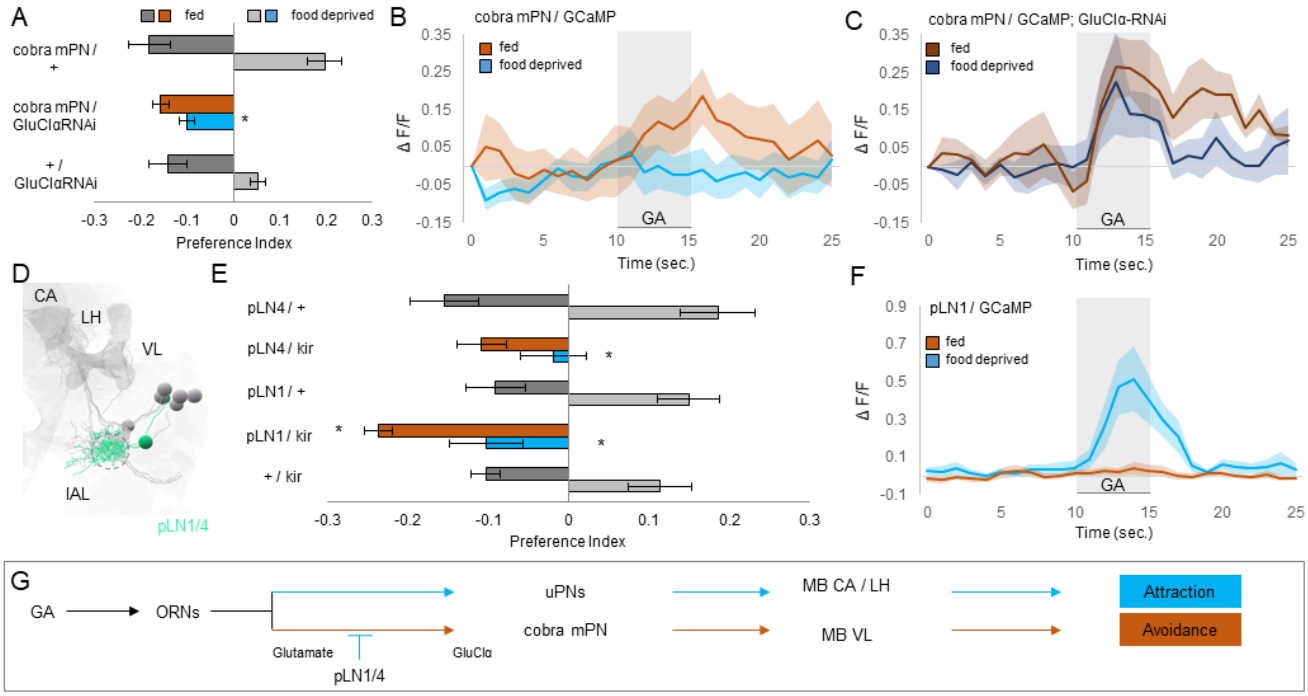

Figure 2. Upon food deprivation, the mPN pathway receives glutamatergic inhibition from pLNs. A Knockdown of the GluClα-receptor using RNAi in cobra mPN has no effect on odor avoidance in the fed state (Kruskal-Wallis test, $p > 0.05$). Odor attraction in the food-deprived state is impaired (Kruskal-Wallis test, post-hoc pairwise comparison, $p < 0.001$) ($n = 4$–8). **B, C** Calcium activity in the cobra mPN in response to GA (10^{-5}). Odor was presented for 5 s. Light colors: The cobra mPN shows decreased activity in the food-deprived state. Dark colors: When expressing GluClα RNAi, we cannot detect any state dependent inhibition ($n = 8$). **D, E** pLNs are lAL local interneurons. Blocking output of pLN1 slightly increases avoidance in the fed state (Kruskal-Wallis test, post-hoc comparison, $p < 0.05$ (pLN1), $p > 0.5$ (pLN4). Blocking pLN1 and 4 leads to loss of attraction in the food-deprived state (Kruskal-Wallis test, post-hoc comparison, $p < 0.05$). ($n = 8$–10). **F** Calcium activity in pLN1 in response to GA (10^{-6}). Odor was presented for 5 s. The pLN1 shows increased activity in the food-deprived state ($n = 7$). **G** pLNs are glutamatergic and provide inhibition onto cobra mPN by GluClα-receptor binding in the lAL. Bar graphs represent pooled data from 5 min to 15 min during testing (mean $\pm$ SEM). Abbreviations: CA, mushroom body calyx; lAL, larval antennal lobe; LH, Lateral Horn; VL, mushroom body vertical lobe.

This phenotype was also obtained by cell-specific knockdown of serotonin synthesis in CSD and exhibited by serotonin mutants (Fig. 3H; S4E).

CSD receives a few synapses from ORNs, but also substantial indirect olfactory input from neurons in the LH that integrate signals from uPNs (Berck et al., 2016). We measured GA-evoked calcium dynamics in CSD, and found an elevation in food-deprived animals compared to fed animals (Fig. 3I; S4F). To determine whether elevated CSD activity could be linked to a change in behavior, we used optogenetics. We expressed the red-sensitive optogenetic effector CsChrimson::mVenus in CSD and tested behavior. Fed larvae that normally show GA avoidance will exhibit attraction when CSD is artificially activated by continuous illumination with red light (Fig. 3J; S5A). We note that basal locomotion patterns (e.g., lengths of crawling movements) are unaffected by CSD activation. CSD affects olfactory valence, but not the ability to crawl towards an olfactory cue (Fig. S5B).

A molecular method to elevate CSD serotonergic release is to inhibit the serotonin transporter SerT, which localizes in presynaptic membranes and recycles released neurotransmitter (Giang et al., 2011). RNAi knockdown of SerT in CSD reduced GA avoidance in fed larvae (Fig. S4G). In contrast, overexpression of SerT (which presumably lowers serotonergic transmission) causes GA avoidance in both fed and food-deprived larvae (Fig. S4G). These phenotypes are consistent with optogenetic activation of CSD and constitutive inactivation of CSD, respectively. These phenotypes also argue against the possibility that state-dependent plasticity occurs in the projection neurons themselves, e.g., by changes in receptor expression.

Notably, the wiring diagram reveals no direct synapses from CSD to the uPNs (Fig. 4A/B). One possibility is that 5-HT7 receptors in the uPNs might be activated by extrasynaptic release or synaptic spillover after food deprivation (Trueta and De-Miguel, 2012; De-Miguel and Trueta, 2005) (Fig. 3K).

Food-deprivation modulates inhibitory interactions in the pLN pathway

Our results suggest that a pLN circuit regulates mPN activity by providing glutamatergic inhibition in the food-deprived state. But what inactivates the pLN1/4 in the fed state? The wiring diagram suggests that pLNs inhibit one another: pLN1/4 receives glutamatergic inhibition from pLN0 (Berck et al., 2016) (Fig. 4B). We were not able to study pLN0 owing to the absence of a cell-specific driver. However, we found that reducing GluClα expression in pLN1 and pLN4 eliminates GA avoidance in the fed state (Fig. S6A/B). Thus, pLN1/4 receive glutamatergic inhibition presumably from pLN0 only when larvae are fed.

Additionally, the local interneurons of the lAL express an inhibitory serotonergic receptor, 5-HT1A (Huser et al., 2017) (Fig. S6C). When we removed the 5-HT1A receptor from the pLN1/4s using CRISPR/Cas9, fed larvae also did not avoid GA (Fig. S6D). According to the wiring diagram, the pLN1/4s receive direct synaptic inputs from CSD that seem to provide

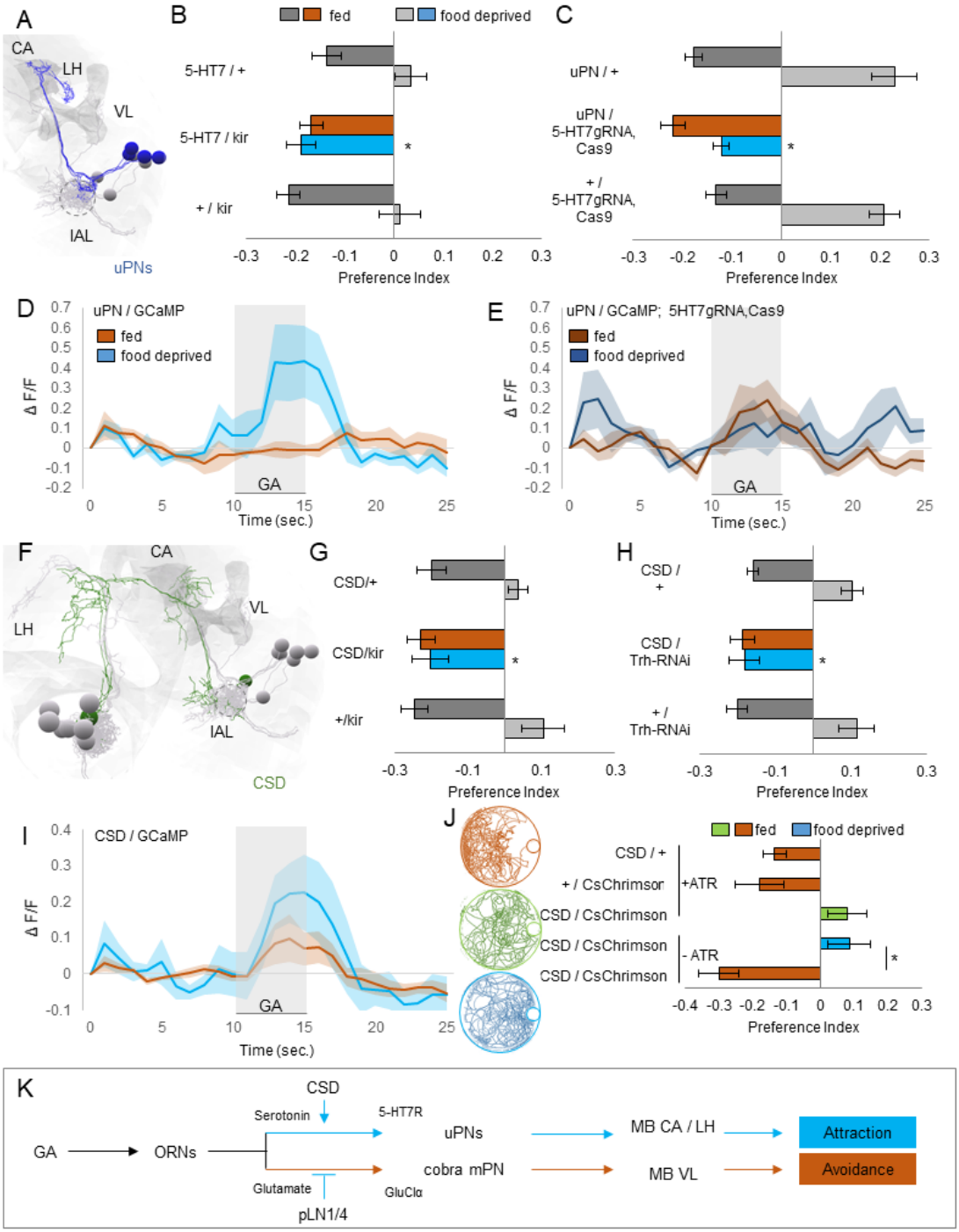

Figure 3. Upon food deprivation, CSD elevates uPN activity via the excitatory 5-HT7 receptor. A, B Blocking neuronal output of 5-HT7 receptor-expressing neurons (*5-HT7-GAL4*, including uPNs) with *UAS-Kir2.1* does not affect odor avoidance in fed larvae (one-way ANOVA, $p > 0.05$); however, odor attraction in food-deprived larvae is impaired (one-way ANOVA, post-hoc pairwise comparison, $p < 0.01$). ($n = 8$). **C** Knockdown of the 5-HT7 receptor with *UAS-Cas9* in the uPNs (*GH146-GAL4*) does not affect odor avoidance in fed larvae (one-way ANOVA, post-hoc pairwise comparison, $p > 0.05$), however odor attraction in food-deprived larvae is impaired (one-way ANOVA, post-hoc pairwise comparison, $p < 0.001$) ($n = 8$–14). **D,E** Calcium activity in the uPNs in response to GA (10^{-6}). Odor was presented for $5\,\mathrm{sec}$. Light colors: The uPNs show increased activity in the food-deprived state. Dark colors: When knocking down the 5-HT7 receptor with *UAS-Cas9* in the uPNs, we cannot detect any state dependent increase in response ($n = 6$–7). **F,G** Blocking neuronal output of the CSD neuron (*R60F02-GAL4*) via expression of *UAS-Kir2.1*, we find no effect on behavior in the fed state (one-way ANOVA, $p > 0.05$). However, food-deprived larvae do not switch their behavior towards attraction (Kruskal-Wallis test, post-hoc pairwise comparison, $p < 0.05$). ($n = 6$–8). **H** Preventing serotonin synthesis in the CSD neuron via expression of *UAS-Trh-RNAi* does not affect odor avoidance in fed larvae (Kruskal-Wallis test, $p > 0.05$). however odor attraction in food-deprived larvae is impaired (Kruskal-Wallis test, post hoc pairwise comparison, $p < 0.01$). ($n = 8$). **I** Calcium activity in the CSD neuron (*R60F02-GAL4*) in response to GA (10^{-8}). Odor was presented for 5 seconds. The CSD neuron responds stronger to GA in the food-deprived state ($n = 8$–10). **J** Optogenetic activation of the CSD neuron leads to odor attraction in fed larva (one-way ANOVA, post-hoc pairwise comparison, $p < 0.05$) ($n = 12$–20). **K** Higher activity and serotonin release by the CSD neuron lead to higher activation of the uPNs via the excitatory 5-HT7 receptor. This induces odor attraction in the food-deprived state. Bar graphs represent pooled data from $5\,\mathrm{min}$ to $15\,\mathrm{min}$ during testing (mean $\pm$ SEM). Abbreviations: CA, mushroom body calyx; IAL, larval antennal lobe; LH, Lateral Horn; VL, mushroom body vertical lobe.

enough serotonin in the fed state to achieve this inhibition (Fig. 4A). Thus, in the fed state, pLN1/4 receive joint inhibition from glutamatergic and serotonergic signals, thereby lowering their ability to inhibit the mPN pathway for odor avoidance (Fig. S6E).

In the food-deprived state, pLN1/4 receive less glutamater-

gic inhibition from pLN0, allowing the mPN pathway to be downregulated. Both inhibitory inputs seem to be required, since increased serotonergic inhibition from CSD in the food-deprived state appears not to be sufficient to inactivate pLN1/4 (Fig. S6D).

All five pLNs originate from the same neuroblast lineage (Berck et al., 2016; Das et al., 2013). Thus, pLN0 might also express the 5-HT1A inhibitory receptor similar to pLN1/4, and might thus be plausibly inactivated by CSD in food-deprived larvae.

A computational model of the state-dependent switch in olfactory valence

To integrate our findings about cellular and synaptic properties with observed network dynamics in different behavioral states, we turned to computational modeling. The wiring diagram reveals the complete synaptic connectivity between all neurons that we studied (Fig. 4A/B). Here, we have uncovered the sign of the connectivity of the glutamatergic and serotonergic pathways in the circuit. To determine whether the dynamics of the circuit would give rise to decision-making, namely the appropriate shift of lAL output between the uPN and mPN pathways, we built a simple dynamical model of the circuit. The weight of every synaptic connection is inferred from the number of synapses between cell types (Berck et al., 2016) (Fig. 4B). The only plausible cellular input to pLN1/4 that provides glutamatergic inhibition is the pLN0. pLN0, like pLN1/4, is modeled as receiving direct serotonergic inhibition from CSD.

Simulation of the model with the known connectivity and synaptic properties indeed reveals a bimodal switch. Elevation of CSD activity in the food-deprived state shifts activity towards the uPN pathway both directly through serotonergic excitation as well as indirectly through recruitment of glutamatergic inhibition of the mPN pathway (Fig. S7). In contrast, weak CSD activity in the fed state shifts activity towards the mPN pathway.

Our model also allows us to test the consequence of all of the molecular and cellular perturbations that we performed to uncover circuit properties. We simulated the effects of removing individual neurons from the circuit (akin to chronic inactivation by Kir2.1) as well as individual synapses (akin to receptor knockdown or knockout), and found that, in every case, we could predict whether the circuit would be shifted towards the uPN or the mPN pathway in either fed or food-deprived animals (Fig. 4C). Taken together, these data suggest that our minimal circuit model is sufficiently comprehensive to produce the key state-dependent modulations. Modeling also defines a computational motif that effectively computes a binary, state-dependent decision by a small wiring diagram.

Discussion

Innate olfactory preferences depend on feeding state

We find that *Drosophila* larvae exhibit innate avoidance of GA in the fed state but innate attraction in the food-deprived state. We also reproduced our key observations about GA using menthol, the only other odor that we found to evoke consistent innate avoidance in fed larvae (Fig. S8A-G). Both odors are common to green leaves. Green leaves are not a preferred food source of the larva, but their odor becomes attractive to food-deprived animals.

We have shown that the assignment of odor valence occurs in the antennal lobe. The behavioral switch from negative valence in fed animals to positive valence in food-deprived animals involves a shift in the relative activity of two lAL output pathways. uPNs are needed for odor attraction, and project to the mushroom body calyx and the lateral horn. The cobra mPN is needed for odor avoidance, and projects to the vertical lobe of the mushroom body. Understanding how these output pathways organize locomotory behavior toward or away from odors will require mapping downstream pathways to the motor circuit. However, we show that the key switch between these output pathways is implemented by the glutamatergic and serotonergic circuitry of the antennal lobe. The fixed architecture of the antennal lobe has long been thought to provide stereotyped formatting of olfactory inputs for downstream circuits (e.g., normalization (Olsen and Wilson, 2008)). Also, assignment of innate olfactory valence has long been thought to occur in the lateral horn (Strutz et al., 2014). Here, we find that the antennal lobe itself is a *bona fide* decision-making center.

CSD, a prominent serotonergic neuron spanning the olfactory system, drives the state-dependent change in serotonergic modulation of the uPN and mPN output pathways. CSD exhibits greater odor-evoked activity in the food-deprived state than in the fed state. When an animal is food-deprived, high levels of serotonin released from CSD both activate the uPN pathway (via the excitatory 5-HT7 receptor) and increase glutamatergic inhibition onto the mPN pathway (via inhibitory glutamatergic local interneurons). There are no direct synapses from CSD onto the uPNs, thus serotonergic transmission likely involves either synaptic overspill or non-synaptic neurotransmitter release. Neuromodulation provides a means of functional reconfiguration of circuit activity in a fixed wiring diagram. Bidirectional modulation of behavioral output by serotonin has also been described in adult *Drosophila* behaviors (Xu et al., 2016).

In mammals, homologous 5-HT receptors are known to regulate appetite and seeking/craving behaviors, suggesting a conserved function for serotonergic regulation of behaviors that depend on feeding state (Ebenezer et al., 2007; Hauser et al., 2015). The neural circuit for early olfactory processing in mammals, the olfactory bulb (OB), is strikingly similar in its molecular and circuit architecture to the *Drosophila* antennal lobe (Gaudry, 2018). Here, we have shown that feeding state directly affects odor-evoked responses of CSD, a serotonergic feedback neuron in the larval olfactory system, which thereby modulates the assignment of behavioral valence. In the mouse, serotonergic projection neurons from the raphe nucleus innervate the OB (McLean and Shipley, 1987) and also modulate distinct OB output pathways and local interneurons (Kapoor et al., 2016; Brunert et al., 2016). The circuit logic and behavioral role of serotonergic pathways in mammalian olfaction is not well understood. Our study shows how the neural architecture of a connectome, by systematic consideration of cellular and synaptic properties, is able to produce different network dynamics that underlie different behavioral decisions. Similar architectures may underlie decision-making in other brain circuits where switching between output pathways produces the flexibility of distinct behavioral responses.

ACKNOWLEDGEMENTS

We would like to thank members of the Samuel and de Bivort labs, as well as Venkatesh Murthy, Armin Bahl, Dana Galili and Benjamin Kottler for comments on

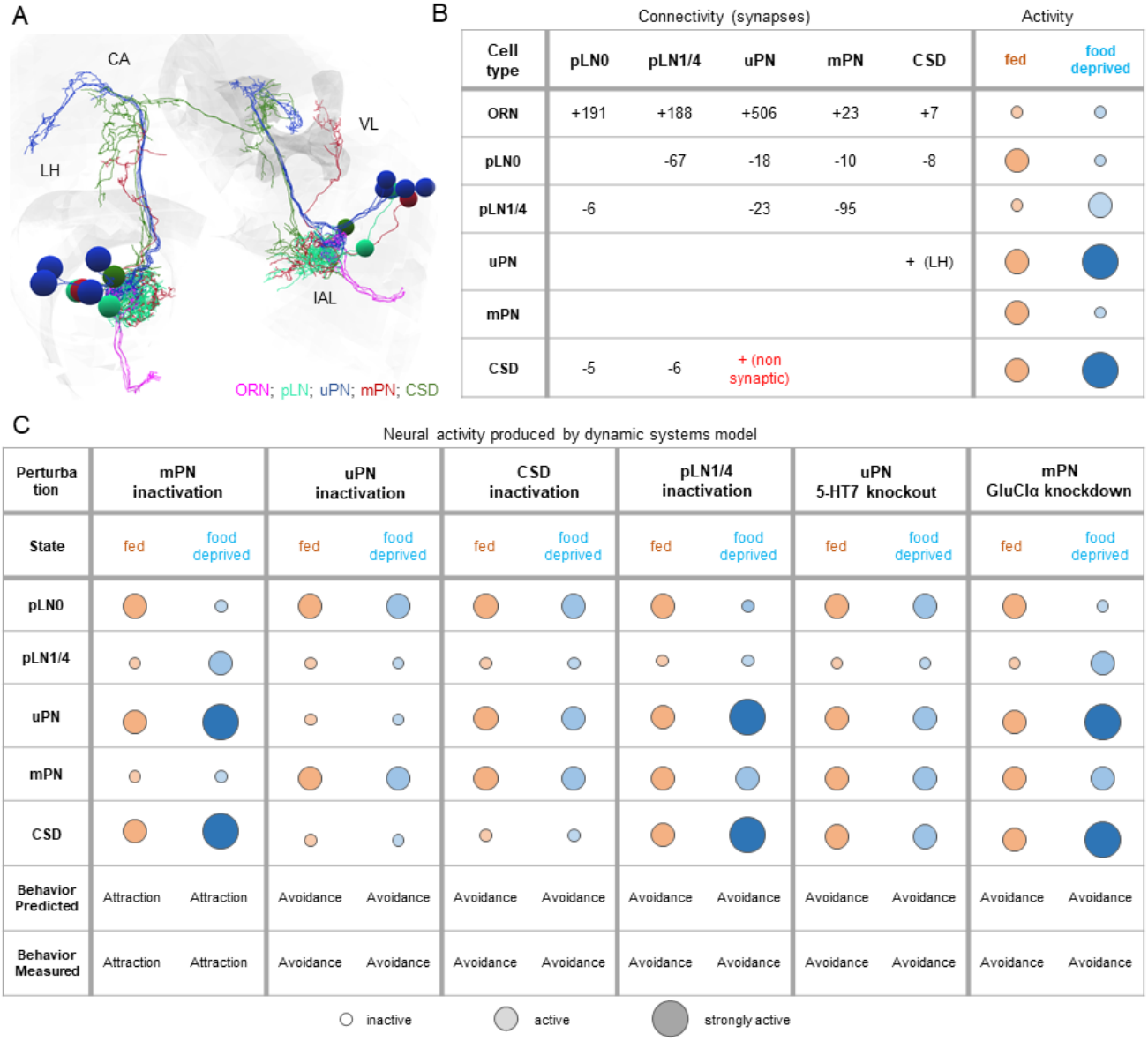

Figure 4. A simple dynamical model recapitulates state-dependent changes in odor valence. A EM reconstructions of all studied neurons in the larval brain. The right mushroom body is shaded gray. Abbreviations: CA, mushroom body calyx; IAL, larval antennal lobe; LH, Lateral Horn; VL, mushroom body vertical lobe. **B** EM connectivity of all studied neurons. Number of synapses between cell types. Circles indicate neural activity of all studied IAL neurons based on functional imaging recordings and behavioral experiments (fed [orange] vs. food-deprived [blue]). In the fed state, the cobra mPN pathway, required for odor avoidance, is active, because cobra mPN does not receive inhibition from pLN1/4s. Upon food deprivation, serotonergic modulation mediated by CSD increases and uPNs receive extrasynaptic modulation via the excitatory 5-HT7 receptor. The mPN receives glutamatergic inhibition from pLN1/4s. **C** Neural activity of all studied IAL neurons in fed (orange) and food-deprived state (blue) upon cell manipulations within the dynamical systems model. Bottom rows: Behavioral output is calculated based on activity of the uPNs and the mPN. The model predicts same behavioral output as we found in behavioral experiments.

the study. We also acknowledge the Bloomington *Drosophila* Stock Center (NIH P40OD018537), Michael Pankratz and James Truman for fly lines. Brian Smith kindly provided odorants. K.V. was supported by a DFG research fellowship (project number 345729665). C.P. acknowledges support by the NIH. A.D.T.S. is supported by grants from the NSF and NIH.

AUTHOR CONTRIBUTIONS

K.V. performed behavioral experiments, functional imaging, anatomical characterization and optogenetics. D.M.Z. performed functional imaging. M.S. and M.R. provided genetic reagents. K.M. performed behavior experiments. L.H.N. analyzed data from optogenetic experiments. S.Q. and C.P. designed the dynamical systems model. A.C. provided access to connectomic data. K.V. conceived the project. K.V. and A.D.T.S. designed research, interpreted the results, and wrote the manuscript with input from all authors.

COMPETING INTERESTS

The authors declare no competing interests.

Methods

Experimental model

Flies were reared at 22 °C under a 12:12 light-dark cycle and 60% humidity in vials containing standard cornmeal agar-based medium. For larval experiments, adult flies were transferred to larvae collection cages (Genesee Scientific) containing grape juice agar plates and 180 mg of fresh yeast paste per cage. Flies were allowed to lay eggs on the agar plate for 1–2 days before the plate was removed for collection of larvae in the different developmental stages. Behavioral experiments were performed with L2 larvae (3–4 days after egg laying), unless otherwise stated (Fig. S2A). Calcium imaging experiments and anatomical studies were performed in L1 larvae (2 days after egg laying). Most transgenic stocks were obtained from Bloomington

Drosophila Stock Center (BDSC, see Table 1).

Cell-specific CRISPR/Cas9-mediated knockout

We generated *UAS-gRNA* lines targeting the 5-HT7 and 5-HT1A receptors, as described previously (Port and Bullock, 2016). In short, we digested the pCFD6 vector (a gift from Simon Bullock, Addgene #73915) with BbsI (New England Biolabs, NEB) and used a Gibson Assembly (NEB) to incorporate PCR products. We generated two PCR fragments each harboring three guide sequences with homology to the CDS of either *5-HT7* or *5-HT1A* (see Table 2). The resulting colonies were sequenced and the correct constructs were inserted into the *attP1* landing site on chromosome II (BDSC #8621) by ΦC31-mediated recombination (Rainbow Transgenic Flies, Camarillo, CA, USA). Transgenic flies were back-crossed to w^{1118} and balanced using BDSC #3703 (Schlichting et al., 2019; Delventhal et al., 2019).

Behavioral assays

Pure odorants were diluted in deionized (DI) water and stored for no more than one week. Our initial screen of behavioral responses in fed larvae involved an odorant panel of natural constituents of ripe fruit from Brian Smith (based on Keesey et al., 2015) (Fig. S1A). Each odorant and odor dilution was stored in the dark and in a separate glass bottle to avoid contamination. For behavior experiments, the following odorants were obtained from Sigma-Aldrich and used at the indicated dilutions (v/v): geranyl acetate, 10^{-4} (except see Fig. S2B; CAS #105-87-3); menthol, 10^{-3} (CAS #89-78-1); ethyl acetate, 10^{-6} (CAS #141-78-6). The larval olfactory choice assay is illustrated in Fig. 1A. For the measurement of olfactory responses in the fed state, 3–4-day-old larvae were picked from grape juice plates and briefly washed in several DI water droplets right before the experiment. For odor preference test in the food-deprived state, larvae were picked from grape juice plates 5–7 h before test (except as otherwise stated, Fig. S2C), washed in DI water droplets and placed in a small Petri dish (VWR, #60872-306, 60 mm × 15 mm) with a 2% agarose plate on the bottom covered by a thin layer of tap water. Before odor preference test, food-deprived larvae were placed in DI water droplets similar to larvae freshly picked from food. At the start of the test, 15 larvae were placed on the surface of a 2% agarose pad in the center of a 10 cm Petri dish equipped with a 12 mm plastic cup at one edge (VWR, #25384-318). Before each experiment, the cup was loaded with 200 µL of odor solution. Larvae were free to explore the arena with closed lid for 15 min. Over time, we counted the number of larvae in each quadrant of the arena, and computed a preference index:

$$\mathrm{PI} = \frac{Q_+ - Q_-}{N},$$

where Q_+ represents the number of larvae in the quadrant containing the odor cup, Q_- represents the number of larvae in the opposite quadrant, and N represents the total number of larvae in the arena.

Each odor preference test used freshly picked and previously untested larvae. Different larvae were tested under fed and food-deprived conditions. Experiments were performed at room temperature under uniform illumination with a point light source (desk lamp) on a clean bench, except for the optogenetic experiments shown in Fig. 3J (see below). In all experiments, we alternated the position of the odor cup in the Petri dish between the left or right sides to avoid systematic bias.

Optogenetics

For optogenetic experiments with CsChrimson, experimental larvae additionally received food supplemented with 0.1 mM all-trans-retinal (ATR; Sigma-Aldrich, CAS #116-31-4). Larval collection cages and grape juices plates were wrapped in foil and kept in dark during egg laying and larval development (Hernandez-Nuñez et al., 2015). Experiments were performed in a lightproof box. Olfactory response behavior was recorded at 4 Hz using a CCD Mightex camera equipped with a long-pass infrared filter (cutoff 740 nm). Larvae received 500 Hz pulsed stimulation with spatially uniform red light (625 nm, pulse width 20 µs, $0.62\,\mathrm{W/m^2} \pm 0.5\,\%$) to activate the optogenetic effector throughout the entire 15 min test period. Larval trajectories were analyzed with custom tracking software (Gershow et al., 2012). For each frame, the number of larvae in the two halves of the Petri dish was analyzed automatically. The preference index was calculated as

$$\mathrm{PI} = \frac{S_+ - S_-}{N},$$

where S_+ represents the number of larvae on the half side containing the odor cup, S_- represents the number of larvae on the opposite side, and N represents the total number of larvae in the arena. The *PI* over each min of the test was pooled for comparable representation of data in Fig. S5A.

Functional imaging with microfluidic device

We used a previously described method for microfluidics and imaging (Si et al., 2019). An 8-channel microfluidic chip was used in this study to deliver odor solutions to an intact larva. The same odors were used as in the behavior setup, however at lower concentrations (GA: 10^{-8}, 10^{-6}, 10^{-5}; menthol: 10^{-4}). Stimuli consisted of 5 s odor pulses interleaved with 15 s water washout periods. L1 larvae were loaded into the microfluidic device using a 1 mL syringe filled with Triton X-100 (0.1% [v/v]) solution. The larva was pushed to the end of the loading channel with its dorsal side closest to the objective. GCaMP signal was recorded using an inverted Nikon Ti-E spinning disk confocal microscope with a 60X water immersion objective (NA 1.2). A CCD microscope camera (Andor iXon EMCCD) captured frames at 30 Hz. The CSD neuron and projection neurons were recorded by scanning the entire volume (step size 1.5 µm) of the brain, ranging from the antennal lobe to the processes in the higher brain. Orco::RFP was used to locate the lAL. Recordings from at least 5–9 larvae were collected for each genotype and condition. All samples were used for analysis unless dendritic varicosities developed in the ORNs over the course of the recording, a sign of unhealthy neurons likely due to mechanical stress.

Anatomical studies

GFP expression patterns of GAL4 and split-GAL4 lines were imaged in intact larvae using an inverted Nikon Ti-E spinning disk confocal microscope with a 60X water-immersion objective (NA 1.2) or 20X objective. To immobilize larvae, they were squeezed between two glass slides using a micromanipulator. Orco::RFP was used to locate the lAL.

Table 1. Fly lines used in this study

Line	Source
Orco^{1}	BDSC #23129
GH146-GAL4	BDSC #30026
GMR32E03-GAL4	BDSC #49716
UAS-Kir2.1	BDSC #6596
Orco-GAL4	BDSC #23292
Or82a-GAL4	BDSC #23125
Or45a-GAL4	BDSC #9975
UAS-GCaMP6m; *Orco::RFP*	This study (*UAS-GCaMP6m*, BDSC #42748; *Orco::RFP*, BDSC #63045)
UAS-GluClα-RNAi (TRiP HMC03585)	BDSC #53356
pLN1-GAL4 (split)	This study (*GMR21D06-AD*, BDSC #70117; *GMR50A06-DBD*, BDSC #68988)
pLN3-GAL4 (split; SS004499)	J. Truman (*GMR42E06-AD*, BDSC #71054; *GMR12C03-DBD*, BDSC #70429)
pLN4-GAL4 (split; SS001730)	J. Truman (*GMR21D06-AD*, BDSC #70117; *GMR12C03-DBD*, BDSC #70429)
UAS-mCD8::GFP; *Orco::RFP*	BDSC #63045
5-HT7–GAL4	M. Pankratz (Becnel et al., 2011)
UAS-gRNA–5-HT7; *UAS-Cas9*	This study (Rosbash lab)
GMR60F02-GAL4	BDSC #48228
UAS-Trh-RNAi (TRiP JF01863)	BDSC #25842
UAS-CsChrimson::mVenus	BDSC #55136
Trh-GAL4	BDSC #38389
DDC-GAL4	BDSC #7009
Trh^{c01440}	BDSC #10531
UAS-SerT	BDSC #24464
UAS-SerT-RNAi (TRiP HMJ30062)	BDSC #62985
5-HT1A–GAL4	M. Pankratz (Luo et al., 2012)
UAS-gRNA–5-HT1A; UAS-Cas9	This study (Rosbash lab)
$y^{1}w^{67c23}$; *P{CaryP}attP1*	BDSC #8621
w^{1118}; sna^{Sco} It^{1}/CyO; MKRS/TM6B	BDSC #3703

Table 2. Guide sequences

gRNA	Sequence
5-HT1A guide 1	TAGCGAACAGCATGAATGAC
5-HT1A guide 2	TGTCATAGCGGCCATTATCC
5-HT1A guide 3	ACGACCGCGACCCGTCGATG
5-HT7 guide 1	CACAGAAACCACAGAACCCA
5-HT7 guide 2	GCATCACCAGCAGCAATTT
5-HT7 guide 3	GGATCTCTGTGTGGCTCTTC

Quantification and statistical analysis

Imaging data were analyzed with custom scripts written in MATLAB, available at *https://github.com/samuellab/Larval-ORN*. Data from behavioral experiments were analyzed with LabVIEW, MATLAB and Microsoft Excel. Data were tested for normality (Shapiro-Wilk test) and analyzed by parametric or non-parametric statistics as appropriate: the Kruskal-Wallis test or one-way analysis of variance (ANOVA). For post-hoc pairwise comparisons, the one- or two-sample t-test, Welch's t-test, or Mann-Whitney U-test were performed as appropriate. The significance level of statistical tests was set to $\alpha = 0.05$. Only the most conservative statistical result of multiple pairwise comparisons is indicated. No statistical methods were used to determine sample sizes in advance, but sample sizes are similar to those reported in other studies in the field. Sample sizes ("n"), p values, and other relevant test statistics are shown in the appropriate figure legends.

Computational circuit model

To better understand how the neural circuitry in the lAL dictates the state-dependent shift of odor valence, we built a dynamical model based on connectomic data and neural activity of larval neurons. We assume that the neural activities for pLNs and cobra mPN are binary (0 and 1), while uPN and CSD neurons have three states, 0, 1, and 2. We denote the state of a neuron at time point t as $S_i(t) \in \{0,1,2\},\ i = 1,\cdots,5$. For simplicity, we have pooled pLN1 and pLN4 (pLN1-4). The synaptic weights and other interactions are grouped as "strong" (with absolute strength 1) and "weak" (with absolute strength w), as shown in Table 3. Based on experimental data, feedback from CSD to uPN is strong after food deprivation, hence we modeled this non-synaptic interaction by setting a weight from CSD to uPN

Table 3. Connection weights ($\boldsymbol{W}$) modeling synaptic and non-synaptic interactions (top five rows), and ORN and basal input of each neuron ($\boldsymbol{I}_{\mathrm{ORN}}^{\top}$ and $\boldsymbol{I}_{\mathrm{basal}}^{\top}$ respectively, bottom two rows)

	pLN0	pLN1-4	uPN	mPN	CSD
pLN0	0	-1	-1	$-w$	$-w$
pLN1-4	$-w$	0	$-w$	-1	0
uPN	0	0	0	0	1
mPN	0	0	0	0	0
CSD	$-\beta$	$-w$	$\{0,2\}$	0	0
ORN	1	1	1	w	w
basal	0	0	0	α	0

to be 2, i.e., $W(5,3) = 2$ under food deprivation. CSD inhibits pLN0 through serotonin, modeled by parameter β. Cobra mPN shows stronger activation in the fed state and thus receives basal input α. As seen in Table 3, a neuron receives several inputs: from ORN, pLN, CSD or baseline input. We can write it in the vector notation:

$$\boldsymbol{h} = \boldsymbol{I}_{\text{ORN}} + \boldsymbol{W}^{\top}\boldsymbol{S} + \boldsymbol{I}_{\text{basal}}, \tag{1}$$

where $\boldsymbol{I}_{\text{ORN}}$ is the input vector from ORNs, $\boldsymbol{I}_{\text{basal}}$ is the basal input vector, and $\boldsymbol{W}$ is the interaction matrix between pLNs, PNs and CSD. The ith neuron's state in the next time step is determined by the total input h_i it receives via the following rule:

$$S_i(t+1) = \begin{cases} 1, & h_i(t) > 0 \\ 0, & h_i(t) \leq 0 \end{cases}$$

for $i = 1,2,4$ (corresponding to pLN0, pLN1-4 and mPN), or

$$S_i(t+1) = \begin{cases} 0, & h_i(t) \leq 0 \\ 1, & 0 < h_i(t) < 2 \\ 2, & h_i(t) \geq 2 \end{cases}$$

for $i = 3,5$ (corresponding to uPN and CSD).

To fit our model parameters, we used the steady state activity at the fed state and food-deprived state of the wild-type larvae from experiments, shown in Table 4.

Table 4. Activity patterns of neurons in fed and food-deprived state of larvae

	pLN0	pLN1-4	uPN	mPN	CSD
Fed	1	0	1	1	1
Food-deprived	0	1	2	0	2

These neural activity patterns are stable and hence impose a constraint on the model parameters w, α, β by

$$\begin{cases} 0 < w < \frac{1}{2} \\ 0 < \alpha \leq 1 - w \\ \frac{1-w}{2} \leq \beta < 1. \end{cases} \tag{2}$$

Consideration of perturbation experiments further constrain the upper bound on β, $\beta < 1 - w$. In our model, we choose a set of parameters that fulfills all the constraints: $w = 0.25$, $\alpha = 0.5$, $\beta = 0.5$.

To relate neural activity to behavioral readout (preference index), we assume a binary readout is determined by

$$\text{PI} = \begin{cases} 1, & S_{\text{uPN}} - 3S_{\text{mPN}} > 0, \\ -1, & S_{\text{uPN}} - 3S_{\text{mPN}} < 0. \end{cases}$$

The exact value of the prefactor before S_{mPN} does not matter, as long as it is larger than 2. Thus, when mPN is on it generates avoidance behavior, otherwise the fly larvae is attracted by the odor. Our model correctly predicts all the behavioral output of perturbation experiments (Fig. 4C).

References

Becnel, J., Johnson, O., Luo, J., Nässel, D. R., and Nichols, C. D. The serotonin 5-HT7dro receptor is expressed in the brain of drosophila, and is essential for normal courtship and mating. *PLoS ONE*, 6(6), 2011. ISSN 19326203. doi: 10.1371/journal.pone.0020800.

Berck, M. E. M., Khandelwal, A., Claus, L., Hernandez-Nuñez, L., Si, G., Tabone, C. J. C. C. J., Li, F., Truman, J. J. W., Fetter, R. D. R., Louis, M., Samuel, A. A. D. D. T., and Cardona, A. The wiring diagram of a glomerular olfactory system. *eLife*, 5(MAY2016):1–21, may 2016. ISSN 2050084X. doi: 10.7554/eLife.14859. URL https://elifesciences.org/content/5/e14859https://elifesciences.org/articles/14859.

Brunert, D., Tsuno, Y., Rothermel, M., Shipley, M. T., and Wachowiak, M. Cell-type-specific modulation of sensory responses in olfactory bulb circuits by serotonergic projections from the raphe nuclei. *Journal of Neuroscience*, 36(25):6820–6835, jun 2016. ISSN 15292401. doi: 10.1523/JNEUROSCI.3667-15.2016.

Chung, B. Y., Ro, J., Hutter, S. A., Miller, K. M., Guduguntla, L. S., Kondo, S., and Pletcher, S. D. Drosophila Neuropeptide F Signaling Independently Regulates Feeding and Sleep-Wake Behavior. *Cell Reports*, 19(12):2441–2450, jun 2017. ISSN 22111247. doi: 10.1016/j.celrep.2017.05.085. URL http://dx.doi.org/10.1016/j.celrep.2017.05.085https://linkinghub.elsevier.com/retrieve/pii/S2211124717307593.

Crossley, M., Staras, K., and Kemenes, G. A central control circuit for encoding perceived food value. *Science Advances*, 4(11):1–12, 2018. ISSN 23752548. doi: 10.1126/sciadv.aau9180. URL http://advances.sciencemag.org/cgi/content/short/4/11/eaau9180.

Dacks, A. M., Christensen, T. A., and Hildebrand, J. G. Phylogeny of a serotonin-immunoreactive neuron in the primary olfactory center of the insect brain. *The Journal of Comparative Neurology*, 498(6):727–746, oct 2006. ISSN 0021-9967. doi: 10.1002/cne.21076. URL http://doi.wiley.com/10.1002/cne.21076.

Das, A., Gupta, T., Davla, S., Prieto-Godino, L. L., Diegelmann, S., Reddy, O. V., Raghavan, K. V., Reichert, H., Lovick, J., and Hartenstein, V. Neuroblast lineage-specific origin of the neurons of the Drosophila larval olfactory system. *Developmental Biology*, 373(2):322–337, jan 2013. ISSN 1095564X. doi: 10.1016/j.ydbio.2012.11.003.

De-Miguel, F. F. and Trueta, C. Synaptic and Extrasynaptic Secretion of Serotonin. *Cellular and Molecular Neurobiology*, 25(2):297–312, apr 2005. ISSN 0272-4340. doi: 10.1007/s10571-005-3061-z. URL http://link.springer.com/10.1007/s10571-005-3061-z.

Delventhal, R., O'Connor, R. M., Pantalia, M. M., Ulgherait, M., Kim, H. X., Basturk, M. K., Canman, J. C., and Shirasu-Hiza, M. Dissection of central clock function in Drosophila through cell-specific CRISPR-mediated clock gene disruption. *eLife*, 8:23–26, oct 2019. ISSN 2050-084X. doi: 10.7554/eLife.48308. URL https://elifesciences.org/articles/48308.

Ebenezer, I., Arkle, M., and Tite, R. 8-Hydroxy-2-(di-N-propylamino)-tetralin (8-OH-DPAT) inhibits food intake in fasted rats by an action at 5-HT1A receptors. *Methods and Findings in Experimental and Clinical Pharmacology*, 29(4):269, 2007. ISSN 0379-0355. doi: 10.1358/mf.2007.29.4.1075362. URL http://journals.prous.com/journals/servlet/xmlxsl/pk{_}journals.xml{_}summary{_}pr?p{_}JournalId=6{&}p{_}RefId=1075362{&}p{_}IsPs=N.

Ganjewala, D. and Luthra, R. Geranyl acetate esterase controls and regulates the level of geraniol in lemongrass (Cymbopogon flexuosus nees ex steud.) mutant cv. GRL-1 leaves. *Zeitschrift fur Naturforschung - Section C Journal of Biosciences*, 64(3-4):251–259, 2009. ISSN 09395075. doi: 10.1515/znc-2009-3-417.

Gaudry, Q. Serotonergic modulation of olfaction in rodents and insects. *Yale Journal of Biology and Medicine*, 91(1):23–32, 2018. ISSN 00440086.

Gershow, M., Berck, M., Mathew, D., Luo, L., Kane, E. A. E., Carlson, J. J. R., and Samuel, A. A. D. T. Controlling airborne cues to study small animal navigation. *Nature methods*, 9(3):290–6, mar 2012. ISSN 1548-7105. doi: 10.1038/nmeth.1853. URL http://www.pubmedcentral.nih.gov/articlerender.fcgi?artid=3513333{&}tool=pmcentrez{&}rendertype=abstract.

Giang, T., Rauchfuss, S., Ogueta, M., and Scholz, H. The serotonin transporter expression in Drosophila melanogaster. *Journal of Neurogenetics*, 25(1-2):17–26, 2011. ISSN 01677063. doi: 10.3109/01677063.2011.553002.

Hauser, S. R., Hedlund, P. B., Roberts, A. J., Sari, Y., Bell, R. L., and Engleman, E. A. The 5-HT7 receptor as a potential target for treating drug and alcohol abuse. *Frontiers in Neuroscience*, 8, jan 2015. ISSN 1662-453X. doi: 10.3389/fnins.2014.00448. URL http://journal.frontiersin.org/article/10.3389/fnins.2014.00448/abstract.

Hernandez-Nuñez, L., Belina, J., Klein, M., Si, G., Claus, L., Carlson, J. R., and Samuel, A. D. T. Reverse-correlation analysis of navigation dynamics in Drosophila larva using optogenetics. *eLife*, 4(MAY):9, aug 2015. ISSN 2050084X. doi: 10.7554/eLife.06225. URL http://dx.doi.org/10.7554/eLife.06225.

Huser, A., Rohwedder, A., Apostolopoulou, A. A., Widmann, A., Pfitzenmaier, J. E., Maiolo, E. M., Selcho, M., Pauls, D., von Essen, A., Gupta, T., Sprecher, S. G., Birman, S., Riemensperger, T., Stocker, R. F., and Thum, A. S. The Serotonergic Central Nervous System of the Drosophila Larva: Anatomy and Behavioral Function. *PLoS ONE*, 7(10):e47518, oct 2012. ISSN 1932-6203. doi: 10.1371/journal.pone.0047518. URL https://dx.plos.org/10.1371/journal.pone.0047518.

Huser, A., Eschment, M., Güllü, N., Collins, K. A. N., Böpple, K., Pankevych, L., Rolsing, E., and Thum, A. S. Anatomy and behavioral function of serotonin receptors in Drosophila melanogaster larvae. *PLOS ONE*, 12(8):e0181865, aug 2017. ISSN 1932-6203. doi: 10.1371/journal.pone.0181865. URL http://dx.plos.org/10.1371/journal.pone.0181865.

Inagaki, H. K., Panse, K. M., and Anderson, D. J. Independent, reciprocal neuromodulatory control of sweet and bitter taste sensitivity during starvation in Drosophila. *Neuron*, 84(4):806–820, nov 2014. ISSN 10974199. doi: 10.1016/j.neuron.2014.09.032. URL http://dx.doi.org/10.1016/j.neuron.2014.09.032http://linkinghub.elsevier.com/retrieve/pii/S0896627314008526https://linkinghub.elsevier.com/retrieve/pii/S0896627314008526.

Johnson, O., Becnel, J., and Nichols, C. D. Serotonin 5-HT2 and 5-HT1A-like receptors differentially modulate aggressive behaviors in Drosophila melanogaster. *Neuroscience*, 158(4):1292–1300, feb 2009. ISSN 03064522. doi: 10.1016/j.neuroscience.2008.10.055. URL https://linkinghub.elsevier.com/retrieve/pii/S0306452208016059http://dx.doi.org/10.1016/j.neuroscience.2008.10.055.

Kapoor, V., Provost, A. C., Agarwal, P., and Murthy, V. N. Activation of raphe nuclei triggers rapid and distinct effects on parallel olfactory bulb output channels. *Nature Neuroscience*, 19(2):271–282, 2016. ISSN 15461726. doi: 10.1038/nn.4219.

Keesey, I. W., Knaden, M., and Hansson, B. S. Olfactory Specialization in Drosophila suzukii Supports an Ecological Shift in Host Preference from Rotten to Fresh Fruit. *Journal of Chemical Ecology*, 41(2):121–128, jan 2015. ISSN 15731561. doi: 10.1007/s10886-015-0544-3.

Kent, K. S., Hoskins, S. G., and Hildebrand, J. G. A novel serotonin-immunoreactive neuron in the antennal lobe of the sphinx moth Manduca sexta persists throughout postembryonic life. *Journal*

of Neurobiology, 18(5):451–465, 1987. ISSN 10974695. doi: 10.1002/neu.480180506.

Kloppenburg, P., Ferns, D., and Mercer, A. R. Serotonin enhances central olfactory neuron responses to female sex pheromone in the male sphinx moth Manduca sexta. *Journal of Neuroscience*, 19 (19):8172–8181, 1999. ISSN 02706474. doi: 10.1523/jneurosci.19-19-08172.1999.

Ko, K. I., Root, C. M., Lindsay, S. A., Zaninovich, O. A., Shepherd, A. K., Wasserman, S. A., Kim, S. M., and Wang, J. W. Starvation promotes concerted modulation of appetitive olfactory behavior via parallel neuromodulatory circuits. *eLife*, 4(JULY2015):1–17, jul 2015. ISSN 2050084X. doi: 10.7554/eLife.08298.001. URL https://elifesciences.org/articles/08298.

Liou, N. F., Lin, S. H., Chen, Y. J., Tsai, K. T., Yang, C. J., Lin, T. Y., Wu, T. H., Lin, H. J., Chen, Y. T., Gohl, D. M., Silies, M., and Chou, Y. H. Diverse populations of local interneurons integrate into the Drosophila adult olfactory circuit. *Nature Communications*, 9(1), 2018. ISSN 20411723. doi: 10.1038/s41467-018-04675-x. URL http://dx.doi.org/10.1038/s41467-018-04675-x.

Liu, W. W. and Wilson, R. I. Glutamate is an inhibitory neurotransmitter in the Drosophila olfactory system. *Proceedings of the National Academy of Sciences of the United States of America*, 110 (25):10294–10299, jun 2013. ISSN 00278424. doi: 10.1073/pnas.1220560110.

Luo, J., Becnel, J., Nichols, C. D., and Nässel, D. R. Insulin-producing cells in the brain of adult Drosophila are regulated by the serotonin 5-HT 1A receptor. *Cellular and Molecular Life Sciences*, 69(3):471–484, feb 2012. ISSN 1420682X. doi: 10.1007/s00018-011-0789-0.

Masuda-Nakagawa, L. M., Gendre, N., O'Kane, C. J., and Stocker, R. F. Localized olfactory representation in mushroom bodies of Drosophila larvae. *Proceedings of the National Academy of Sciences of the United States of America*, 106(25):10314–10319, jun 2009. ISSN 00278424. doi: 10.1073/pnas.0900178106. URL www.pnas.org/cgi/content/full/.

McLean, J. H. and Shipley, M. T. Serotonergic afferents to the rat olfactory bulb: I. Origins and laminar specificity of serotonergic inputs in the adult rat. *The Journal of neuroscience : the official journal of the Society for Neuroscience*, 7(10):3016–3028, 1987. ISSN 02706474. doi: 10.1523/jneurosci.07-10-03016.1987.

Neckameyer, W. S., Coleman, C. M., Eadie, S., and Goodwin, S. F. Compartmentalization of neuronal and peripheral serotonin synthesis in Drosophila melanogaster. *Genes, Brain and Behavior*, 6(8): 756–769, 2007. ISSN 16011848. doi: 10.1111/j.1601-183X.2007.00307.x.

Nichols, C. D. 5-HT2 receptors in Drosophila are expressed in the brain and modulate aspects of circadian behaviors. *Developmental Neurobiology*, 67(6):752–763, may 2007. ISSN 19328451. doi: 10.1002/dneu.20370. URL http://doi.wiley.com/10.1002/dneu.20370.

Olsen, S. R. and Wilson, R. I. Lateral presynaptic inhibition mediates gain control in an olfactory circuit. *Nature*, 452(7190):956–960, mar 2008. ISSN 14764687. doi: 10.1038/nature06864.

Port, F. and Bullock, S. L. Augmenting CRISPR applications in Drosophila with tRNA-flanked sgRNAs. *Nature Methods*, 13(10):852–854, 2016. ISSN 15487105. doi: 10.1038/nmeth.3972.

Python, F. and Stocker, R. F. Immunoreactivity against choline acetyltransferase, γ-aminobutyric acid, histamine, octopamine, and serotonin in the larval chemosensory system of Drosophila melanogaster. *Journal of Comparative Neurology*, 453(2):157–167, 2002. ISSN 00219967. doi: 10.1002/cne.10383.

Root, C. M., Ko, K. I., Jafari, A., and Wang, J. W. Presynaptic Facilitation by Neuropeptide Signaling Mediates Odor-Driven Food Search. *Cell*, 145(1):133–144, apr 2011. ISSN 00928674. doi: 10.1016/j.cell.2011.02.008. URL https://linkinghub.elsevier.com/retrieve/pii/S0022202X15370834https://linkinghub.elsevier.com/retrieve/pii/S009286741100122X.

Roy, B., Singh, A. P., Shetty, C., Chaudhary, V., North, A., Landgraf, M., VijayRaghavan, K., and Rodrigues, V. Metamorphosis of an identified serotonergic neuron in the Drosophila olfactory system. *Neural Development*, 2(1):1–17, 2007. ISSN 17498104. doi: 10.1186/1749-8104-2-20.

Saudou, F., Boschert, U., Amlaiky, N., Plassat, J., and Hen, R. A family of Drosophila serotonin receptors with distinct intracellular signalling properties and expression patterns. *The EMBO Journal*, 11(1):7–17, jan 1992. ISSN 0261-4189. doi: 10.1002/j.1460-2075.1992.tb05021.x.

Schlichting, M., Díaz, M. M., Xin, J., and Rosbash, M. Neuron-specific knockouts indicate the importance of network communication to drosophila rhythmicity. *eLife*, 8:1–20, 2019. ISSN 2050084X. doi: 10.7554/eLife.48301.

Schoofs, A., Hückesfeld, S., and Pankratz, M. J. Serotonergic network in the subesophageal zone modulates the motor pattern for food intake in Drosophila. *Journal of Insect Physiology*, 106 (March 2017):36–46, 2018. ISSN 00221910. doi: 10.1016/j.jinsphys.2017.07.007. URL https://doi.org/10.1016/j.jinsphys.2017.07.007.

Si, G., Kanwal, J. J. K., Hu, Y., Tabone, C. J. C. C. J., Baron, J., Berck, M., Vignoud, G., and Samuel, A. A. D. Structured Odorant Response Patterns across a Complete Olfactory Receptor Neuron Population. *Neuron*, 101(5):950–962.e7, mar 2019. ISSN 08966273. doi: 10.1016/j.neuron.2018.12.030. URL https://doi.org/10.1016/j.neuron.2018.12.030https://linkinghub.elsevier.com/retrieve/pii/S0896627318311504.

Strutz, A., Soelter, J., Baschwitz, A., Farhan, A., Grabe, V., Rybak, J., Knaden, M., Schmuker, M., Hansson, B. S., and Sachse, S. Decoding odor quality and intensity in the Drosophila brain. *eLife*, 3:e04147, 2014. ISSN 2050084X. doi: 10.7554/eLife.04147.

Trueta, C. and De-Miguel, F. F. Extrasynaptic exocytosis and its mechanisms: A source of molecules mediating volume transmission in the nervous system. *Frontiers in Physiology*, 3 SEP (September):1–19, 2012. ISSN 1664042X. doi: 10.3389/fphys.2012.00319.

Wang, Y., Pu, Y., and Shen, P. Neuropeptide-gated perception of appetitive olfactory inputs in drosophila larvae. *Cell Reports*, 3(3):820–830, 2013. ISSN 22111247. doi: 10.1016/j.celrep.2013.02.003. URL http://dx.doi.org/10.1016/j.celrep.2013.02.003.

Wu, Q., Zhao, Z., and Shen, P. Regulation of aversion to noxious food by Drosophila neuropeptide Y- and insulin-like systems. *Nature Neuroscience*, 8(10):1350–1355, oct 2005. ISSN 10976256. doi: 10.1038/nn1540.

Xu, L., He, J., Kaiser, A., Gräber, N., Schläger, L., Ritze, Y., and Scholz, H. A single pair of serotonergic neurons counteracts serotonergic inhibition of ethanol attraction in Drosophila. *PLoS ONE*, 11(12):1–15, 2016. ISSN 19326203. doi: 10.1371/journal.pone.0167518.

Zhang, X. and Gaudry, Q. Functional integration of a serotonergic neuron in the Drosophila antennal lobe. *eLife*, 5(AUGUST):1–24, aug 2016. ISSN 2050-084X. doi: 10.7554/eLife.16836. URL https://elifesciences.org/articles/16836.

Supplemental figures

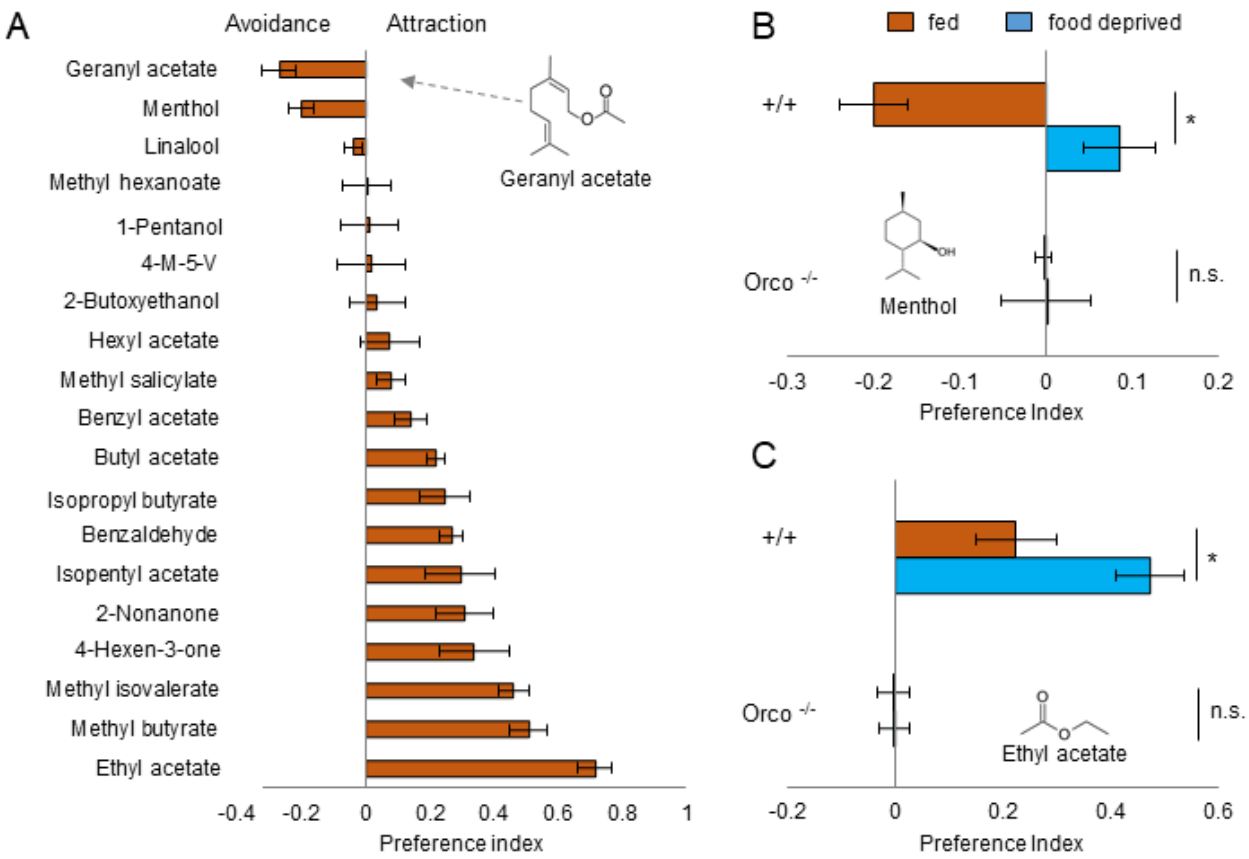

Figure S1. Food deprivation induces a change in olfactory decision making across odorants and is ORN dependent a. Odor screening in fed larvae. Only menthol and geranyl acetate induced aversion, strongest attraction was elicited by ethyl acetate. All odors were tested with 10^{-4} dilution, except menthol (10^{-3}). **b.** Larvae change their response to menthol (conc. 10^{-3}) after food deprivation from avoidance to attraction (two-sample t-test, $p < 0.001$). Mutant larvae (*Orco*$^{-/-}$) that lack functional ORNs do not show any significant response to the odor in the fed and food deprived state (one-sample t-test, $p > 0.05$)($n = 8$). **c.** Larvae show increased attraction to ethyl acetate (conc. 10^{-6}) after food deprivation (two-sample t-test, $p < 0.05$). Mutant larvae (*Orco*$^{-/-}$) that lack functional ORNs do not show any significant response to the odor in the fed and food deprived state (one-sample t-test, $p > 0.05$)(n =6–8).

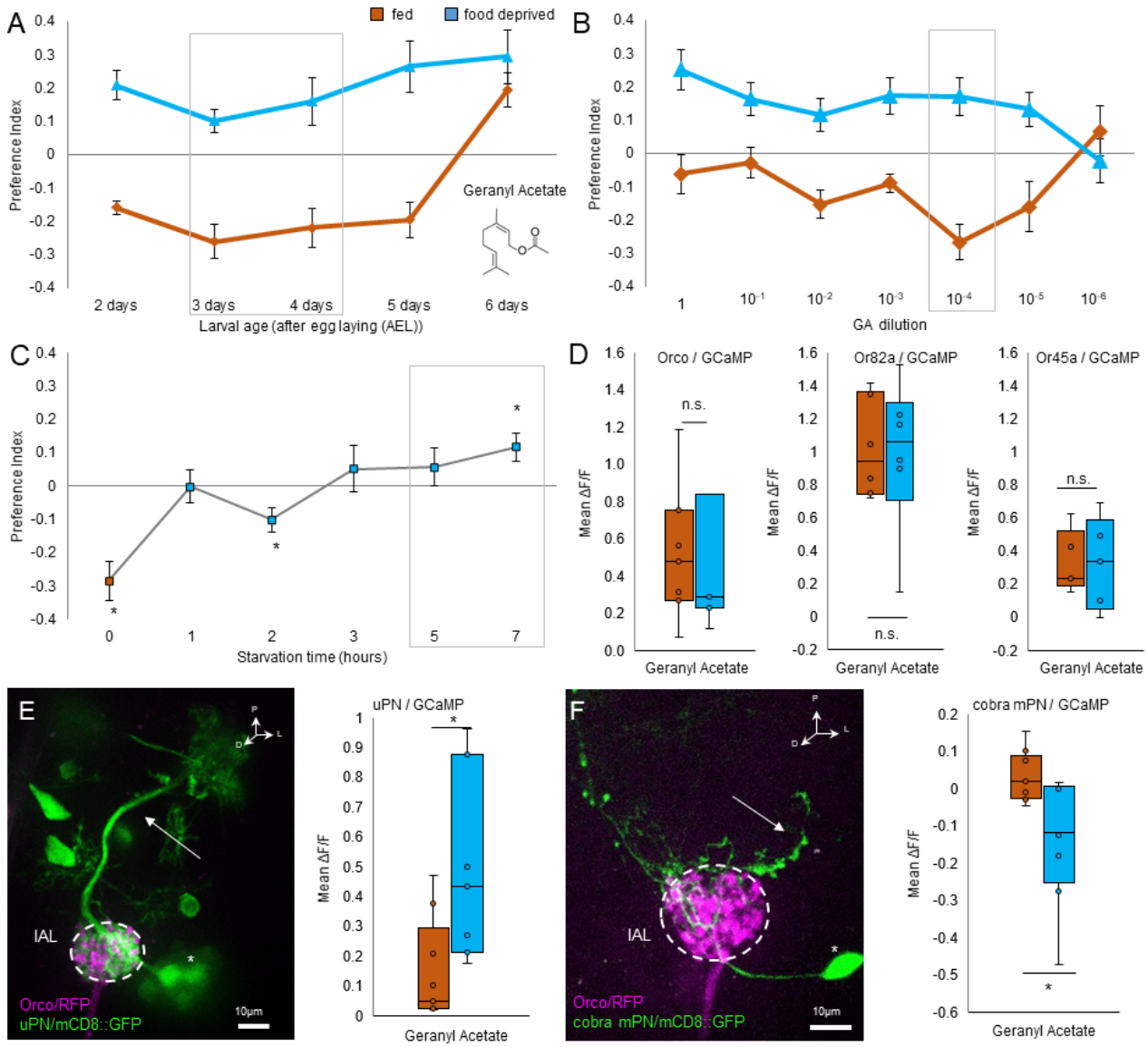

Figure S2. GA behavior is stable across test parameters A The switch in GA response is present over all feeding stages of the larvae (2-5 days AEL, two-sample t-test, $p < 0.001$). Larvae entering the wandering state show attraction also in the fed state (6 days AEL, two-sample t-test, $p > 0.05$). ($n = 8$–10). **B** For each dilution of GA tested, except the lowest (two-sample t-test, $p > 0.05$), we find a significant switch in behavior between states (two-sample t-test, $p < 0.05$, strongest effect for 10^{-4}: two-sample t-test, $p < 0.001$) ($n = 6$–14). **C** Response to GA switches to attraction after food deprivation (one-way ANOVA, $p < 0.001$). In fed state larvae avoid the odor (one sample t-test, $p < 0.001$). After short food deprivation larvae lose the avoidance towards GA (1h, 3h, 5h, one sample t-test, $p > 0.05$) or only slightly avoid it (2h, one sample t-test, $p < 0.05$). They are significantly attracted to the odor after 7 hours of food deprivation (one sample t-test, $p < 0.05$). ($n = 12$-16). **D** Calcium activity in the ORNs in response to GA. Mean change in response normalized to baseline before odor presentation. ORNs respond to GA (10^{-8}) in fed and food deprived state, however there is no change in response upon food deprivation (two-sample t-test, $p > 0.05$). ($n = 7$). The OR82a neuron shows same GA (10^{-6}) response in both states (two-sample t-test, $p > 0.05$) (n=6). The OR45a neuron shows same GA response (10^{-6}) in both states (two-sample t-test, $p > 0.05$) ($n = 5$). **E** *GH146-GAL4* labels uniglomerular projection neurons (uPN line). Arrow indicates axonal projection. Asterisk indicates cell bodies. IAL = larval Antennal Lobe. The uPNs respond stronger to odors in the food deprived state (two-sample t-test, $p < 0.05$). ($n = 7$–9). **F** *GMR32E03-GAL4* labels the cobra mPN. Arrow indicates axonal projection. Asterisk indicates cell body. IAL = larval Antennal Lobe. The cobra mPN is inhibited by odors in the food deprived state (two-sample t-test, $p < 0.05$). ($n = 8$–9). Grey boxes indicate parameters used throughout the study. Bar graphs represent pooled data from 5-15 min during testing (mean $\pm$ SEM).

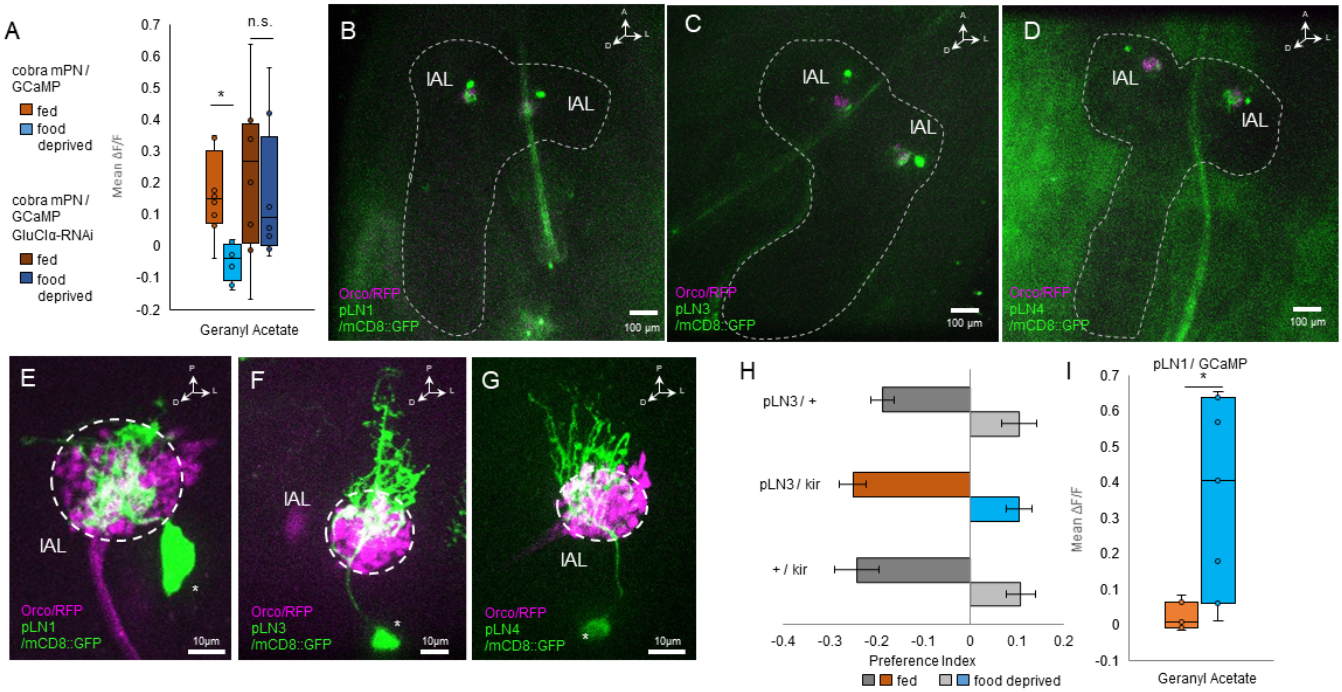

Figure S3. Cobra mPN is inhibited by glutamate released from pLN1,4, but not pLN3 A Calcium activity in the cobra mPN in response to GA. Mean change in response normalized to baseline before odor presentation. Light colors: The cobra mPN is inhibited by GA in the food deprived state (two-sample t-test, $p < 0.01$). Dark colors: Upon GluClα-receptor knockdown the cobra mPN shows same response in both states (two-sample t-test, $p > 0.05$).($n = 8$). **B-D** Whole brain expression patterns of pLN 1, pLN3 and pLN 4 Split-GAL4 lines. Dashed line = larval brain outline. IAL = larval Antennal Lobe. **E-G** Expression patterns of pLN 1, pLN3 and pLN 4 Split-GAL4 lines in the IAL. Asterisks indicate cell bodies. IAL = larval Antennal Lobe. **H** Block of pLN3 has no effect on odor response in both states (one-way ANOVA, $p > 0.05$). ($n = 8$–10) **I** Mean fluorescence change during odor presentation compared to baseline before odor presentation. The pLN1 does not respond to GA (10^{-6}) in the fed state, but shows increased response after food deprivation (two-sample t-test, $p < 0.05$). ($n = 7$). Bar graphs represent pooled data from 5-15 min during testing (mean $\pm$ SEM).

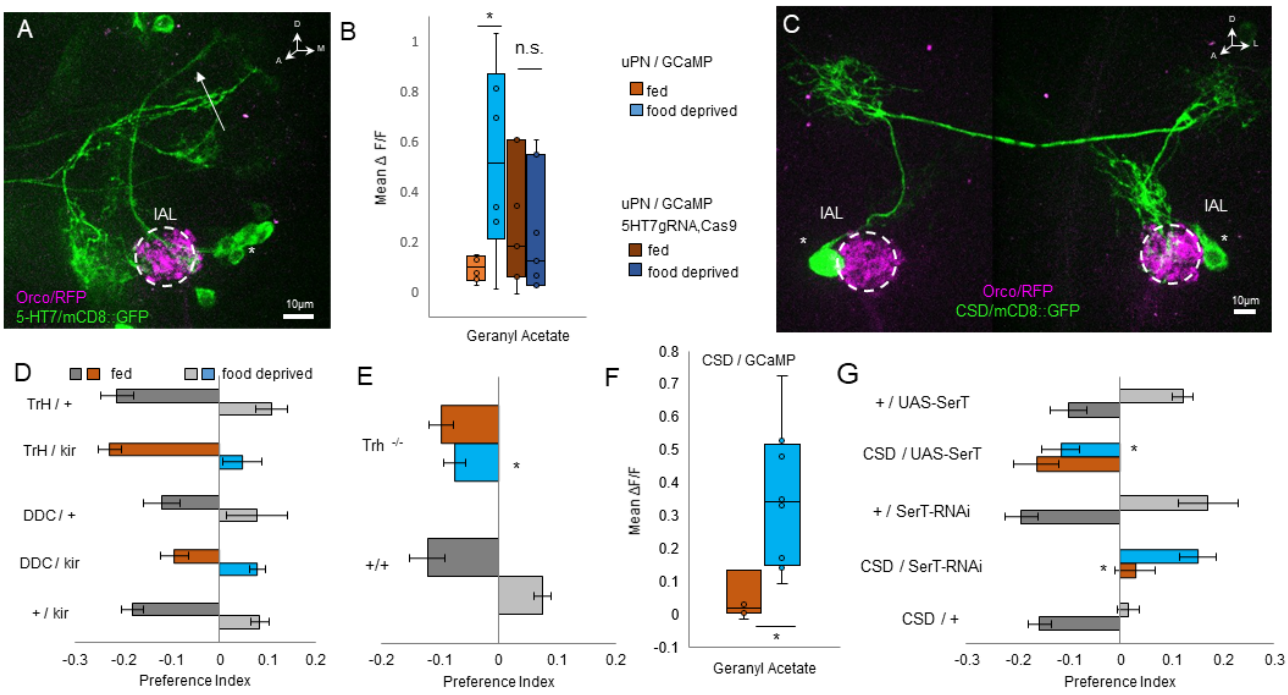

Figure S4. Serotonin released from CSD excites uPNs **A** Expression pattern of 5-HT7-GAL4. uPNs are labeled in the IAL. Arrow indicates axonal projections. Asterisk indicates cell bodies. IAL = larval Antennal Lobe. **B** Calcium activity in the uPNs in response to GA 10^{-6}. Mean change in response normalized to baseline before odor presentation. Light colors: The uPNs show increased response to the odor in the food deprived state (two-sample t-test, $p < 0.05$). Dark colors: Upon knockout of 5-HT7 receptor in the uPNs, they show the same response in both states (two-sample t-test, $p > 0.05$). ($n = 6$–7). **C** *GMR60F02-GAL4* labels the CSD neuron. Asterisk indicates cell bodies. IAL = larval Antennal Lobe. **D** Blocking output of neurons labeled by *Trh-GAL4* does not affect fed (one-way ANOVA, $p > 0.05$) nor food-deprived behavior (one-way ANOVA, $p > 0.05$) towards GA. ($n = 6$–10). Blocking output of neurons labeled by *DDC-GAL4* does not affect fed (one-way ANOVA, $p > 0.05$) nor food-deprived behavior (one-way ANOVA, $p > 0.05$) towards GA. ($n = 6$–14) **E** Mutant larvae (*Trh*$^{-/-}$) unable to synthesize serotonin show normal GA avoidance in fed state similar to control levels (two-sample t-test, $p > 0.05$), however they do not switch to GA attraction after food deprivation (two-sample t-test, $p < 0.01$) ($n = 6$–8). **F** Calcium activity in the CSD neuron in response to GA (10^{-8}). Mean change in response normalized to baseline before odor presentation. The CSD neuron responds stronger to GA in the food deprived state (two-sample t-test, $p < 0.05$). ($n = 8$–10). **G** Upon knockdown of the serotonin transporter in the CSD neuron using SerT-RNAi we see a significant effect in the fed (one-way ANOVA, post hoc pairwise comparison, $p < 0.01$) but not food deprived (one-way ANOVA, post hoc pairwise comparison, $p > 0.05$) state of larvae ($n = 8$–10). Overexpression of the serotonin transporter in the CSD neuron using UAS-SerT leads to a loss of attraction in the food deprived state (one-way ANOVA, post hoc pairwise comparison, $p < 0.01$), however there is no phenotype in the fed state (Kruskal Wallis test, $p > 0.05$). ($n = 8$). Bar graphs represent pooled data from 5-15 min during testing (mean $\pm$ SEM).

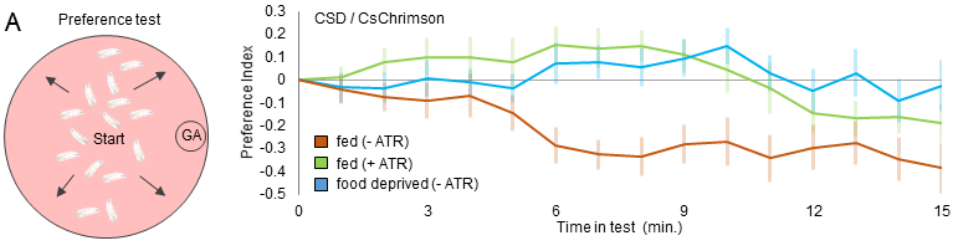

B	CSD/ Chrimson	CSD/ Chrimson	CSD/ Chrimson	+/Chrimson	CSD/+
ATR	-	-	+	+	+
State	fed	food deprived	fed	fed	fed
GA response	Avoidance	Approach	Approach	Avoidance	Avoidance
Run length	●	●	●	●	●
Run speed	●	●	●	●	●
Run duration	●	●	●	●	●

● unchanged ● increased ● decreased

Figure S5. CSD activation affects locomotion parameters differently than food deprivation **A** Activation of the CSD neuron by expressing UAS-Chrimson in a fed larva mimics the food deprived olfactory response behavior. **B** Locomotion parameters of larvae. Food deprived larvae show increased run length due to increased run speed and run duration. Artificial activation of CSD only induces an increase in run duration.

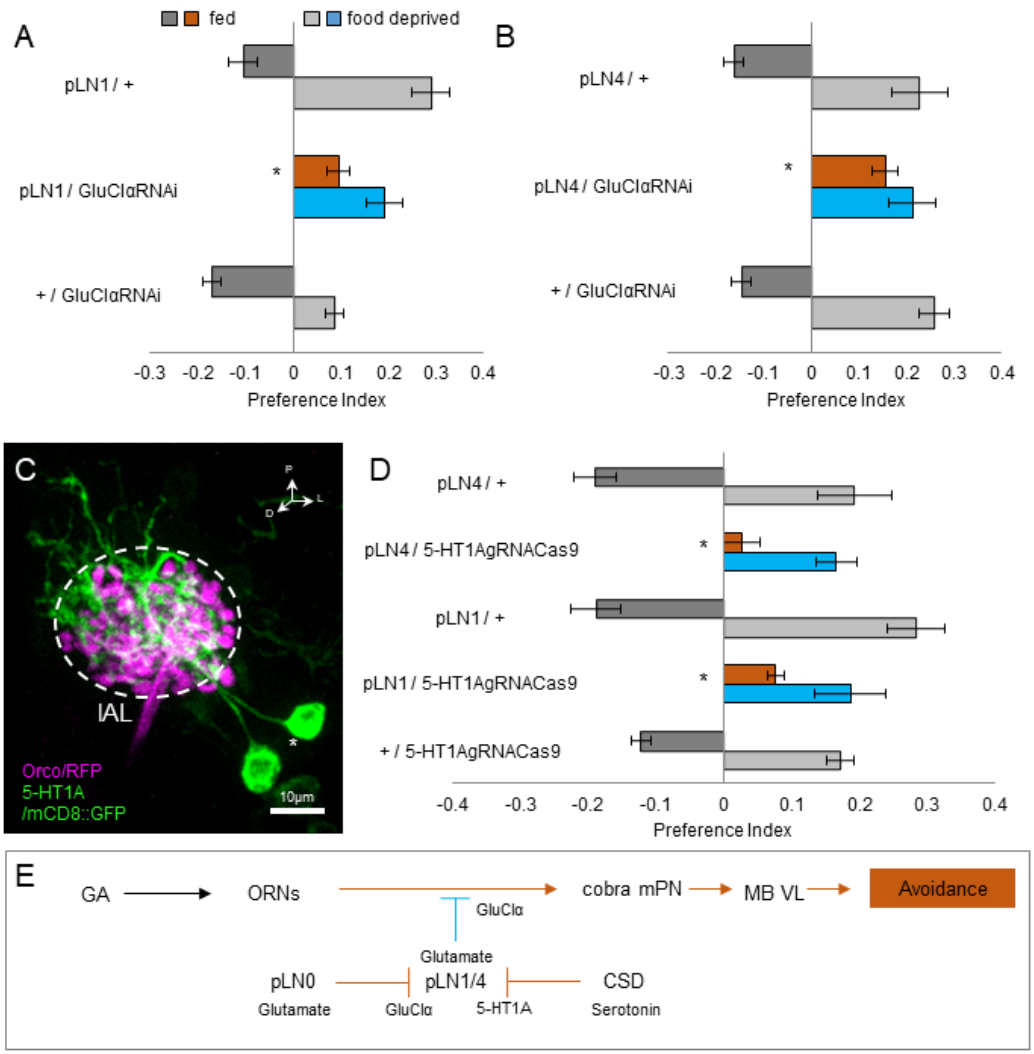

Figure S6. pLN1/4 receive glutamatergic and serotonergic inhibition in the fed state A Expression pattern of *5-HT1A-GAL4*. Two local lAL neurons are labeled. Asterisk indicates cell bodies. lAL = larval Antennal Lobe. **B** Knockdown of the 5HT1A receptor in the picky LNs leads to loss of avoidance in the fed state (one-way ANOVA, posthoc pairwise comparison, $p < 0.001$), however attraction in food deprived state is unaffected (one-way ANOVA, $p > 0.05$). ($n = 6$–16). **C** Knockdown of the GluClα-receptor in pLN1 impairs odor avoidance in the fed state (one-way ANOVA, posthoc pairwise comparison, $p < 0.001$). Odor attraction in the food deprived state is not affected (one-way ANOVA, posthoc pairwise comparison, $p > 0.05$) ($n = 12$–8). **D** Knockdown of the GluClα-receptor in pLN4 neurons impairs odor avoidance in the fed state (one-way ANOVA, posthoc pairwise comparison, $p < 0.001$). Odor attraction in the food deprived state is not affected (one-way ANOVA, $p > 0.05$) ($n = 7$–8). **E** In the fed state, pLN1/4 receive inhibition from a glutamatergic neuron (most likely pLN0) and the serotonergic CSD neuron. Therefore, they are not able to inhibit the downstream cobra mPN. Bar graphs represent pooled data from 5-15 min during testing (mean $\pm$ SEM).

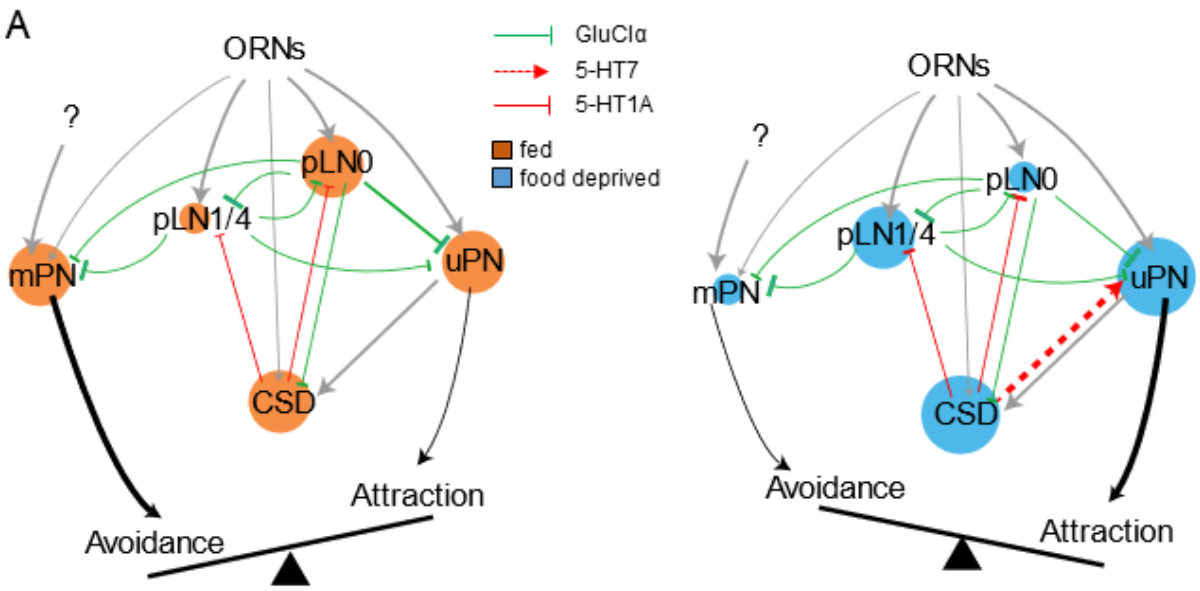

Figure S7. Dynamical systems model connectivity and cell activity A Schematic of model connectivity and neuronal activity in fed (orange) and food deprived (blue) state. Size of circles indicates activity state.

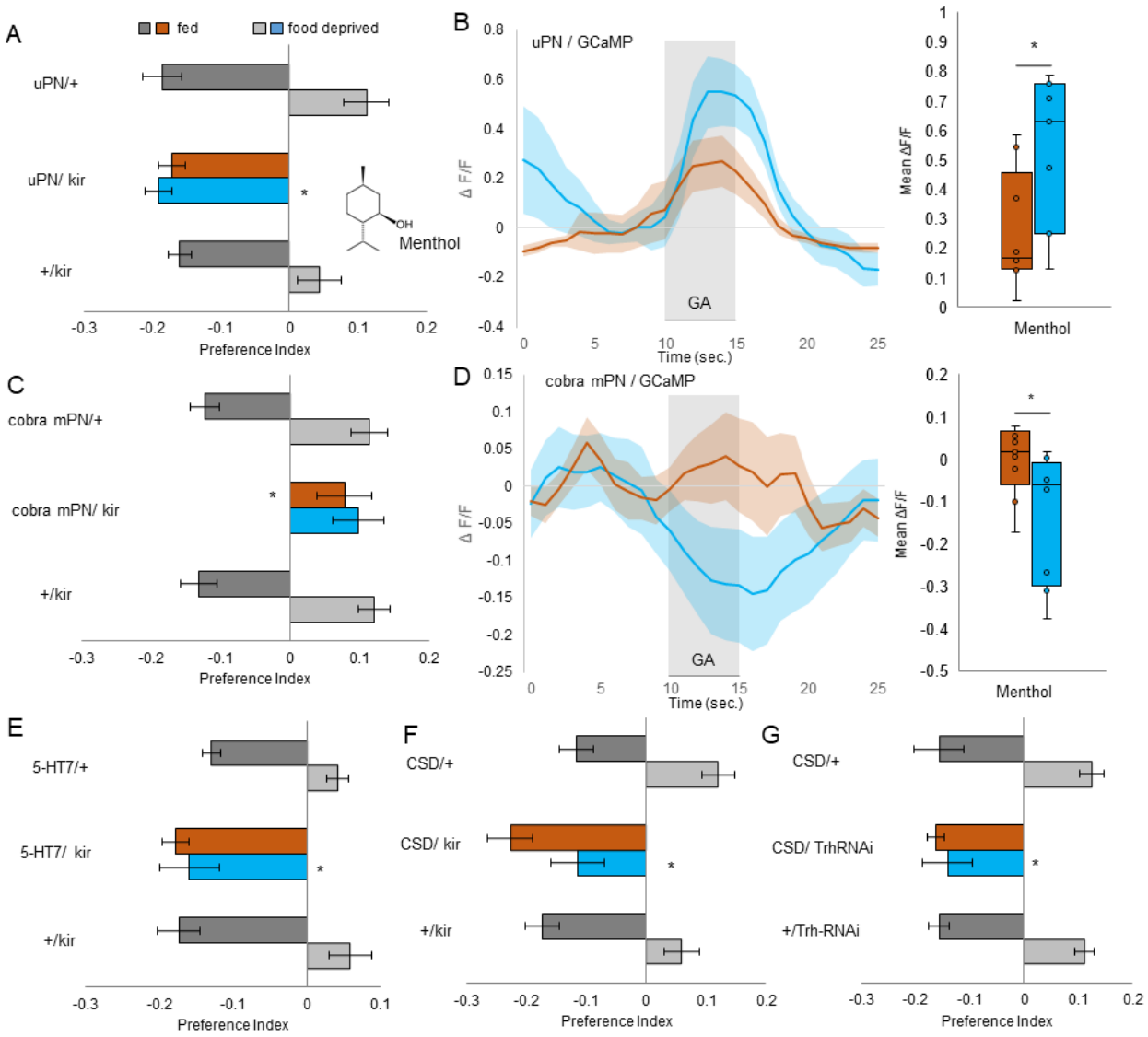

Figure S8. State dependent olfactory behavior towards the odor menthol requires same circuit as for GA A Blocking output of uPNs labeled by *GH146-GAL4* with *UAS-kir2.1* leads to impairment of the food deprived menthol response (one-way ANOVA, posthoc pairwise comparison, $p < 0.001$), but not the fed menthol response (one-way ANOVA, $p > 0.05$). ($n = 4$–6). **B** uPNs show increased response to menthol after starvation (two-sample t-test, $p < 0.05$) ($n = 7$–9). **C** Blocking output of cobra mPN labeled by *GMR32E03-GAL4* leads to impaired odor avoidance in the fed state (one-way ANOVA, posthoc pairwise comparison, $p < 0.01$). However, no effect on odor attraction in the food deprived state can be found (one-way ANOVA, $p > 0.05$). ($n = 6$). **D** After food deprivation, cobra mPN shows decreased response to menthol (two-sample t-test, $p < 0.05$)($n = 8$–9). **E** Blocking output of neurons labeled by *5-HT7-GAL4* with *UAS-kir2.1* leads to impairment of the food deprived menthol response (one-way ANOVA, posthoc pairwise comparison, $p < 0.01$), but not the fed menthol response (one-way ANOVA, $p > 0.05$). ($n = 8$–10). **F** Blocking the output of the CSD neuron with *UAS-kir2.1* has no effect in fed state (one-way ANOVA, $p > 0.05$), but leads to impaired food deprived behavior towards menthol (one-way ANOVA, posthoc pairwise comparison, $p < 0.01$). ($n = 8$–10) **G** Knockdown of serotonin synthesis in the CSD neuron does not affect menthol avoidance in fed state (one-way ANOVA, $p > 0.05$). In food deprived state we see an effect compared to controls (one-way ANOVA, posthoc pairwise comparison, $p < 0.01$). ($n = 8$). Bar graphs represent pooled data from 5-15 min during testing (mean $\pm$ SEM).